Effect of Point Defect Generation on Transient Enhanced Diffusion

by

Desmond Rodney Lim

Submitted to the Department of Electrical Engineering in partial fulfillment of the requirements for the degree of

Master of Science in Electrical Science & Engineering

at the

MASSACHUSETTS INSTITUTE OF TECHNOLOGY

August 6, 1994

Author .....
Department of Electrical Engineering
August 6, 1994

Certified by .....
Conor Rafferty
Member of Technical Staff, AT&T Bell Laboratories
Company Supervisor

Certified by .....
Dimitri A. Antoniadis
Professor, Department of Electrical Engineering
Thesis Supervisor

Accepted by .....
F. R. Morgenthaler
Chairman, Department Committee on Graduate Theses

Effect of Point Defect Generation on Transient Enhanced Diffusion

by

Desmond Rodney Lim

Submitted to the
Department of Electrical Engineering and Computer Science

August 8, 1994

In Partial Fulfillment of the Requirements for the Degree of Master of Science in Electrical Science and Engineering

Abstract

The phenomenon of Transient Enhanced Diffusion (TED), in which boron or phosphorus dopants in silicon diffuse rapidly following ion implantation, is widely believed to be caused by excess interstitials introduced by the implant. However, the physical mechanisms of TED are still not well understood. The interaction of point defects with boron to cause transient enhanced diffusion was examined to help shed light on these models.

Diffusion of boron in silicon at 800°C following silicon damage was studied for very short times. Transient diffusion was found to proceed at a steady rate even at the shortest times. The rate was about 6000 times higher than the equilibrium diffusion rate at the same temperature. A deep boron marker moved at the same rate as a shallow boron marker, providing a lower bound of $10^{-9}cm^2s^{-1}$ for the interstitial diffusivity. The high diffusivity and steady supersaturation of interstitials suggest that interstitial clustering must be taken into account when modeling transient diffusion. Without a mechanism to hold the interstitials in place, the high diffusivity would rapidly reduce the interstitial supersaturation.

Etching the surface to bring it into closer proximity to the damage was shown to reduce the amount of transient diffusion. This supports the idea that the surface is the predominant annealing site for damage after transient diffusion. Finally the effect of vacancy injection, by oxidation in the presence of NF_3, on boron TED was studied. It was shown that at 900°C this process had a negligible effect on TED, while at 1100°C it caused more TED than in the inert controls.

Thesis Supervisor: Dimitri Antoniadis
Title: Professor, Department of Electrical Engineering and Computer Science

Company Supervisor: Conor Rafferty
Title: Member of Technical Staff, AT&T Bell Laboratories

Acknowledgments

I would like to express my deepest gratitude to Conor Rafferty for his insight, patience and guidance. This thesis would have been impossible without Conor's brilliant insight into the material.

I am also indebted to my thesis advisor, Professor Antoniadis, for finding time in his busy schedule to be my thesis advisor and to provide me with valuable input on point defect diffusion.

Amongst the many at Bell Labs who have helped me, I am most grateful to Rodney Kistler and Clifford King. Rod, with his vast knowledge in processing, was extremely helpful when I encountered problems in the design or the running of experiments. In addition to growing CVD samples, Cliff had numerous ideas and ingenious solutions during the planning stages of the experiments. Special thanks also to Mark Pinto, my department head at the Labs, Henry Luftman for SIMS analyses and to Carolyn Flemings for all her wonderful help, both technical and non-technical. I am also grateful to Fred Klemens, for doing such a great job with the RIE, to Marty Green and to Dan Brasen for growing the fluorinated oxides and to Hans Gossman for his automatic diffusivity extracting program.

Over the years, I have received support from my friends and family. I am unable to list all those friends who have helped me remain sane whilst I was working on this thesis. I would like to thank Laura for her helpful suggestions on improving this manuscript.

I am unable to express my gratitude to my parents and my sister Leona in words. They have always motivated me and given me constant encouragement. Without them, I would not have made it this far. Thank you.

Table of Contents

List of Figures

Chapter 1

Introduction

Since the birth of integrated circuits (ICs) in the 1960s, ICs have undergone phenomenal technological improvement. The density and speed of circuits has increased exponentially with time while the cost/bit has decreased almost as rapidly [1]. This inexorable trend of shrinking electronics devices has led some to speculate that by the year 2000, the number of transistors/chip will reach 1 billion devices/chip. However, before that goal is reached, many challenges remain in packaging and processing.

In general, the decreasing size of electronic devices make them more susceptible to higher order phenomena which would have not been critical in the past. For example, the next generation of CMOS devices will require ultra shallow p+ junctions with junction depths of less than 1000 Å to minimize short channel effects and to maintain low contact resistance [2]. These shallow junctions will be difficult to fabricate because ion implantation can cause large amounts of crystal damage both in terms of point defects and extended defects. These defects can, in turn, result in large amounts of extrinsic diffusion in boron and phosphorous, known as Transient Enhanced Diffusion (TED). Since boron is the only viable p+ dopant, this effect has made the task of forming ultra shallow p+/n junctions difficult.

In addition to affecting profiles vertically, ion implantation can affect profiles laterally, on the order of tenths of microns away from the implant. In fact, lateral TED effects due to the source drain ion implants have caused V_t adjustment profiles in MOS devices to shift. This phenomenon has, in turn, resulted in the reverse short channel effect, that is, the anomalous increase in the threshold voltage with the decrease of device dimensions,

accompanied possibly by the degraded channel mobility of these devices [3]. As device dimensions shrink further, these effects will probably become more pronounced.

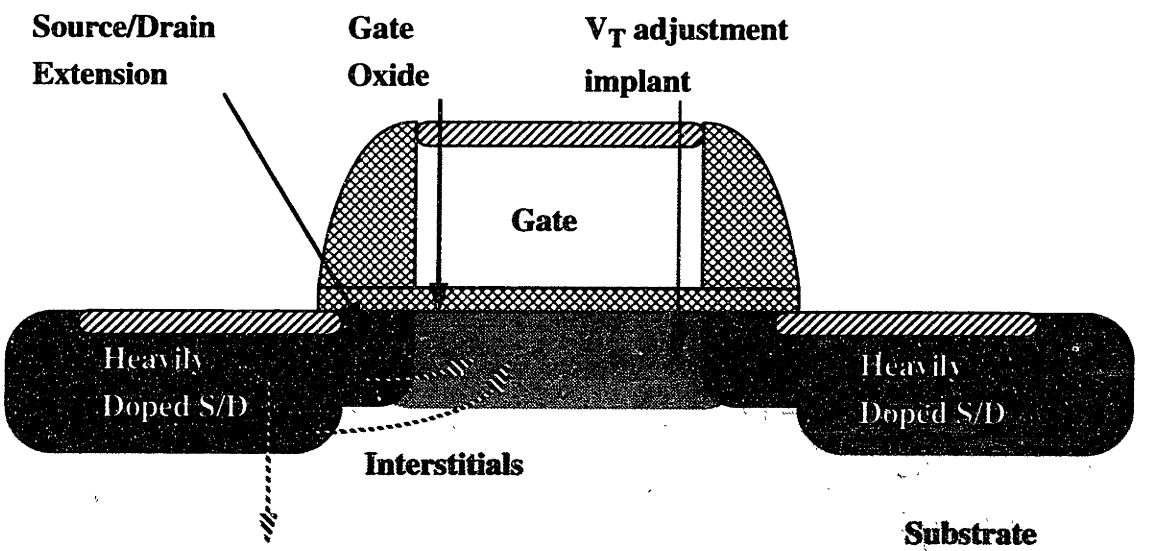

Figure 1.1: Schematic showing how interstitials from source drain and extension implants can affect the V_T implant and source drain profiles.

Thus the objective and motivation of this thesis is to study the effects of point defects on transient enhanced diffusion, with the hope of gaining more insight into point defect diffusion models. Furthermore, I will examine methods of affecting the point defect concentration after implantation, with the hope of reducing the effects of transient enhanced diffusion.

In the next chapter, point defect diffusion models will be described. These point defect diffusion mechanisms are needed in process simulators in order to more accurately model

diffusion. While it is well known that point defects affect the diffusion of substitutional dopants, many aspects of these models are still being hotly debated.

Chapter 3 describes the study of the time evolution of transient enhanced diffusion of boron and will shed light on the annealing kinetics of point defects in silicon damaged by ion implantation. In Chapter 4, the effect of surface proximity to the damage profile induced by ion implantation on transient enhanced diffusion will be studied. Chapter 5 describes the effect of oxidation in the presence of NF_3 on transient enhanced diffusion.

The first two experiments are designed to shed light on the mechanism of point defect interaction with dopants, while the last experiment is designed to test the efficacy of vacancy injection mechanisms on the suppression of transient enhanced diffusion.

Chapter 2

Theory

2.1 Importance of point defects in processing

Point defects, which include vacancies and interstitials, have recently become topics of interest in silicon processing because many processing problems in silicon arise from defects associated with excess interstitials in silicon. For example, these defects cause enhanced diffusion and slow activation of boron. Since boron is currently the only viable p+ dopant in silicon processing, it is essential that we understand its interaction with point defects. Unfortunately, excess interstitials are produced in many processes essential to the fabrication of a VLSI chip. For example, ion implantation produces a vacancy rich layer near the surface and an interstitial-rich region deeper in the bulk [4]. The net result of implant damage is a supersaturation of interstitials which is deeper than the vacancy profile due to knock on effects. See figure 2.1. These excess interstitials may then agglomerate and form dislocation loops such as EOR defects [5].

Processes which produce excess interstitials or interstitial-rich defects are detrimental for three reasons. The first reason is junction leakage. Defects, especially in space charge regions, can result in large leakage currents, which are detrimental for many devices [13]. In addition, dislocations and defects in the space charge region of a Bipolar Junction Transistor (BJT) kills minority lifetime which reduces the gain of the BJT.

The second reason is the slow electrical activation of boron which has been observed after a high dose ion implant [6]. Silicon self-interstitials are thought to compete with interstitial and electrically inactive boron for substitutional sites and are also believed to

act as nucleation sites for boron precipitates to form. Thus, a sample with more interstitials will take a longer time to reach full electrical activation.

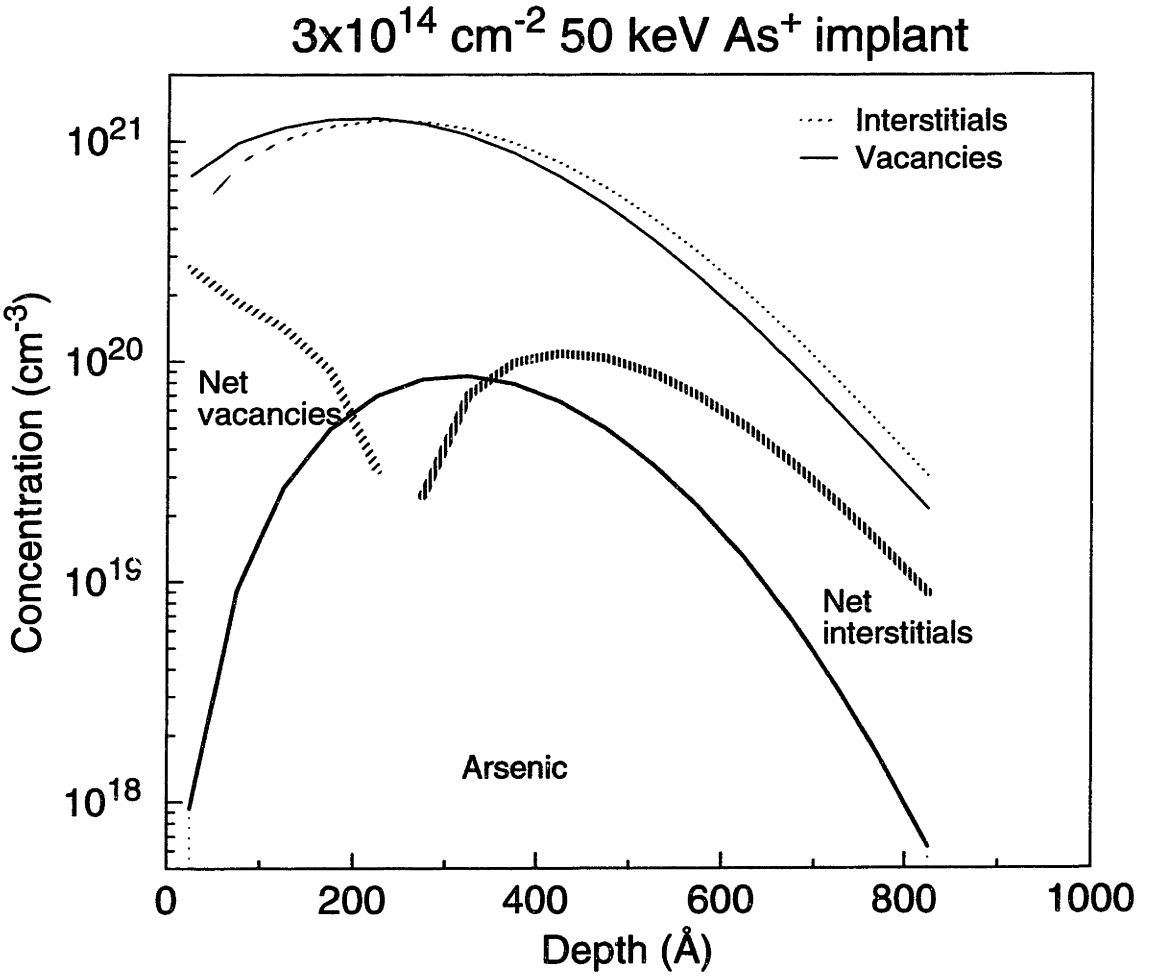

Figure 2.1: Results of Boltzmann simulation showing the interstitial and vacancy concentration due to As ion implantation into Si [8-10].

The third reason, which I will be focussing on, is the enhanced diffusion of boron and phosphorus [7-12] due to interstitials produced by ion implantation and produced during oxidation [1,16-18]. The diffusion of boron is thought to occur by an interstitial mechanism, which means that an increased concentration of interstitials by ion implantation or

interstitial injection during oxidation will result in enhanced boron diffusion. The effect of enhanced diffusion in silicon during oxidation is known as Oxidation Enhanced Diffusion (OED), while the effect of enhanced diffusion which occurs for a short time after ion implantation is known as Transient Enhanced Diffusion (TED). This enhanced diffusion makes implanted boron profiles hard to control and makes shallow implanted boron profiles extremely hard to achieve.

2.2 Point defect diffusion model

It is now widely accepted that in order to simulate diffusion, a model incorporating point defects should be used [15]. These models were first proposed to explain OED [15-18] and have since been applied to explain TED [7-12, 14]. Simulators incorporating such models are important in the design of semiconductor devices, since several design iterations may be performed on the simulator before actual processing. Thus, simulations will yield considerable time and cost savings in the design of the next generation of silicon IC devices.

In the point defect diffusion model, it is assumed that diffusion of a substitutional dopant atom in silicon occurs primarily with the assistance of a point defect. The point defect of interest in silicon is either a silicon interstitial or a vacancy. Antoniadis [18] has shown that the ratio of the diffusivity of a dopant atom D_A to that under intrinsic conditions D_A^* is given by

$$\frac{D_A}{D_A^*} = f_I \frac{C_I}{C_I^*} + (1 - f_I) \frac{C_V}{C_V^*} \tag{2.1}$$

where C_I and C_V are the interstitial and vacancy concentrations respectively. C_I^* and C_V^* are the equilibrium and intrinsic interstitial and vacancy concentrations. Thus, when C_I =

C_I^* and $C_V = C_V^*$, then $D_A = D_A^*$. This equation is valid in the limit where the number of diffusing species (i.e. the point defect dopant complex) is much less than the concentration of the dopants.

The parameter f_I, the fractional interstitialcy diffusion, can be thought of as the fraction of diffusion due to the interstitial component and takes values between 0 and 1. For dopant atoms such as boron which diffuse primarily via the interstitial mechanism, f_I is approximately 1. Hence,

$$\frac{D_{boron}}{D^*_{boron}} \approx \frac{C_I}{C_I^*} \tag{2.2}$$

This implies that the time integrated enhancement of boron under intrinsic conditions at any point in space is given by:

$$\int_t \frac{D_{boron}}{D^*_{boron}} dt \approx \int_t \frac{C_I}{C_I^*} dt \tag{2.3}$$

which is the time integrated supersaturation of interstitials at that point. The left hand side of the equation yields the net boron diffusion. The integral on the right hand side can be calculated numerically and is used to determine the net diffusion in the point defect transient enhanced diffusion simulations which will be presented later. This integral is useful when there is spatial variation in the diffusion enhancement, since the integral can be calculated at any point in space.

Under steady state conditions, by the law of mass action, the product of the interstitial concentration and the vacancy concentration should be a constant, i.e. $C_I C_V = C_I^* C_V^*$. This steady state extrinsic injection occurs during oxidation enhanced diffusion, where the interstitial injection value is not very high and C_I is on the order of 10 C_I^* and the time over which OED occurs is generally much shorter than the time for vacancies and intersti-

tials to reach equilibrium. On the other hand, during implantation, where C_I can be of the order of 1000 C_I^*, it is unclear whether the vacancy and interstitial components can come to equilibrium within the time frame of TED and hence steady state diffusion should not be assumed.

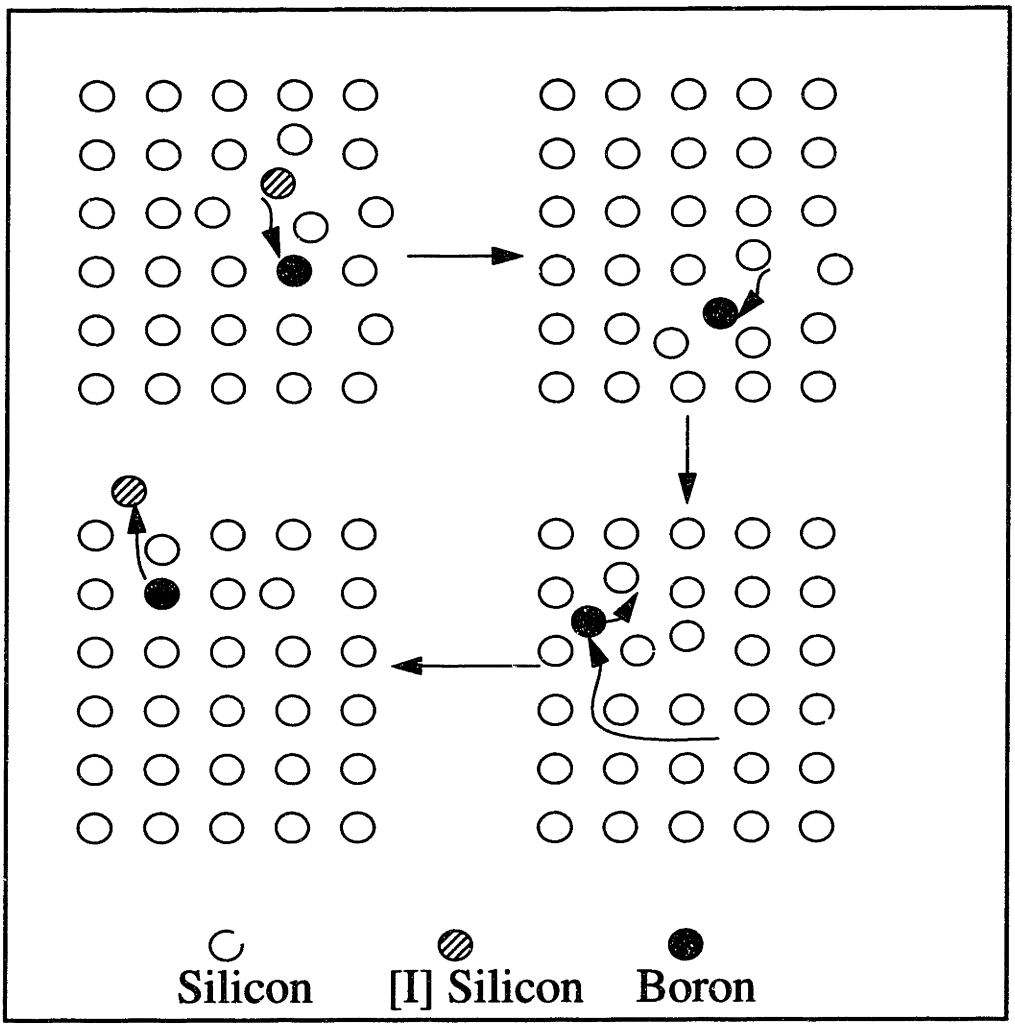

Figure 2.2: Schematic of interstitial diffusion of Boron

2.3 Boron diffusion model in PROPHET

The AT &T simulator, PROPHET, was used to simulate the phenomenon of transient enhanced diffusion [3]. The basic point defect diffusion model used in PROPHET for the

modeling of transient enhanced diffusion effects of boron in silicon solves the following partial differential equations in the bulk:

- the diffusion equation for interstitials:

$$\frac{\partial C_I}{\partial t} = \nabla \cdot \left(D_I C_I^* \nabla \frac{C_I}{C_I^*} \right) - \nabla \bullet F_{BI} - k_{bulk} (C_I C_V - C_I^* C_V^*) \tag{2.4}$$

- the equivalent vacancy diffusion equation,

- the diffusion equation for the B-I and B-V pairs:

$$\frac{\partial C_B}{\partial t} = -\nabla \cdot (F_{BI} + F_{BV}) \tag{2.5}$$

where the point defect flux F_{BI} is:

$$F_{BI} = -D_{BX} e^{-\Psi} \nabla \left(\frac{X}{X^*} C_B e^{\Psi} \right) \tag{2.6}$$

and

F_{BI}= Flux of boron-interstitial complexes

k_{bulk} = bulk recombination coefficient

D_{BXi} = diffusivity of i^{th} charged state

D_{BX} = weighted average of D_{BXi}

X = total number of defects

X^* = total number of defects in equilibrium, i.e.

$$X^* = \sum_{X_i} X_o e^{-\xi_i \Psi}$$

ψ = potential for electric field effects

In addition, there is a boundary condition for the flux at the surface

$$-F_{BI} = -k_{surf} (C_I - C_I^*) + g\,(\text{oxidation rate}) \tag{2.7}$$

where

k_{surf} = surface recombination coefficient

Point defect diffusion will be studied in the intrinsic regime to simplify the problem as this will eliminate the electric field effects as well as concentration dependent effects.

Although the basic point defect model has been presented, additional models have been implemented in order to fully explain transient diffusion. For example, transient enhanced diffusion occurs over a relatively long period of time, on the order of tens of minutes at 800°C, which might suggest that the interstitials diffuse slowly at 800°C to "hang around" long enough to cause this transient. However, there is reason to believe that the interstitial diffusivity, D_I is in fact very large (see chapter three).

In order to explain this rather long anneal time, an interstitial clustering model was implemented. In this model, interstitials produced during ion implantation form clusters and anneal out of these clusters relatively slowly. These clusters may be small interstitial-rich defects like the <311> defect or simply small clusters of 10s of Angstroms in diameter which take some time to anneal out, under diffusion limited conditions. In order to reduce computation time, an equilibrium clustering model of the form [19]:

$$\frac{1}{C_{I,\,mobile}} = \frac{1}{C_I^* K_{clust}} + \frac{1}{C_{I,\,total}} \tag{2.8}$$

is used, where $C_{I,mobile}$ is the mobile interstitial species which will be used in the equation mentioned on the previous page, $C_{I,total}$ is the total interstitial concentration at any point and K_{clust} is a constant such that K_{clust} is greater than or equal to one. Thus when $C_{I,total}$ is much less than $C_I^* K_{clust}$, $C_{I,mobile} \sim C_{I,total}$ and when $C_{I,total}$ is much more than $C_I^* K_{clust}$, $C_{I,mobile} \sim C_I^* K_{clust}$. Thus, one may view $C_I^* K_{clust}$ as the maximum free interstitial concentration and K_{clust} as the maximum enhancement at any given time.

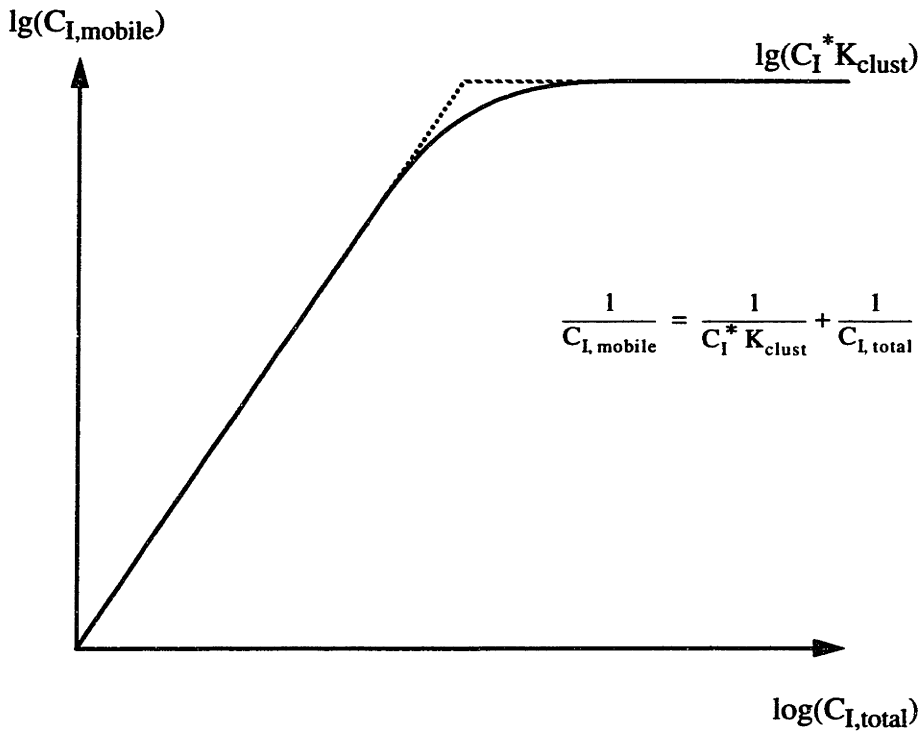

Figure not to scale

Figure 2.3: Transfer function of $C_{I,mobile}$ vs. $C_{I,total}$

For modeling TED of boron in the intrinsic regime, the most important parameters are the diffusion parameters D_I, C_I^*, the recombination parameters K_{surf}, K_{bulk}, the clustering coefficient K_{clust}, the intrinsic boron diffusivity D_{BI}^* and the initial damage distribution. Since it is possible to independently and accurately determine the $D_I C_I^*$ product and the intrinsic boron diffusivity, there are essentially 4 parameters to fit in addition to the initial damage distribution, which will be discussed in the next section. Figure 2.4 shows schematically how these parameters are related to TED.

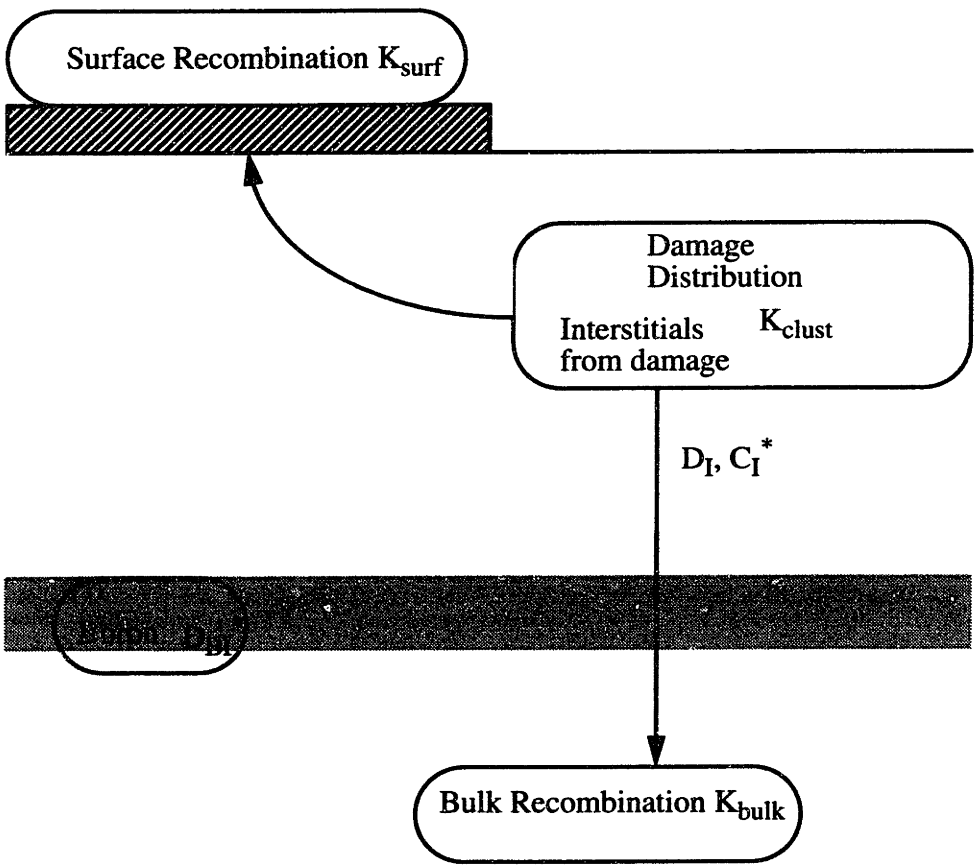

Figure 2.4: Schematic of interstitials interacting with boron to cause transient enhanced diffusion

2.4 Damage distribution, +f model

A discussion of transient enhanced diffusion must also include a discussion of the initial magnitude and distribution of damage caused by the ion implant because the value of extracted parameters such as C_I^*, which cannot be measured accurately in TED type experiments, will depend strongly on the choice of initial implant distribution.

Although the point defect diffusion model is well established, it is still not clear how to model both the initial distribution and the time evolution of point defects introduced by

ion implantation. This is further complicated by the fact that it is difficult to experimentally measure point defect concentrations, so Monte Carlo or Boltzmann Transport Equation based codes [9-10] have been developed to try to understand the initial implant damage profiles. The two techniques agree qualitatively and the resulting damage distribution looks, in general, like the one shown in figure 2.1.

As can be seen from the figure, ion implantation creates a large number of point defects. Most of this damage is in the form of Frenkel pairs, which in all likelihood, rapidly recombine on annealing. Several authors have used this initial distribution as the starting point in their simulations [21]. Although this may seem to be the most accurate and best way to model the initial defect distribution, it has been shown recently that if the damage is adjusted to give the correct channeling characteristics, these models overestimate the damage measured by channeling RBS methods by an order of magnitude [20].

In order to keep the initial damage distribution simple, a modified version of the +1 model, used by Giles [8] is used. The +1 model assumes that each atom implanted into the material contributes one interstitial and that the distribution of the interstitial is the same as that of the implanted species. A further assumption is that the Frenkel pairs which are produced during the implantation are unimportant and rapidly recombine after annealing. The reasoning behind the +1 model is that when an implanted atom becomes substitutional it displaces a silicon atom, which in turn becomes an interstitial; meanwhile the extra Frenkel pairs annihilate.

In the +f model used in this thesis, the number of interstitials each implanted ion contributes is a fitted parameter, f, of order one. Furthermore, it is assumed that these interstitials cluster up very rapidly during the post implant anneal and that the phenomenon of transient enhanced diffusion is a result of the slow dissolution of these clusters.

There are several reasons why f may not be equal to one. One reason which will tend to reduce f, and hence the number of interstitials which are clustered, is the process of interstitials diffusing rapidly away from the damaged region before they are able to cluster. These interstitials may recombine either at the surface or in the bulk or they may be trapped in defects like dislocations loops which are stable over the time frame of TED. This process of rapid interstitial diffusion will compete with the clustering of interstitials from Frenkel pairs, since the latter reaction will tend to increase f.

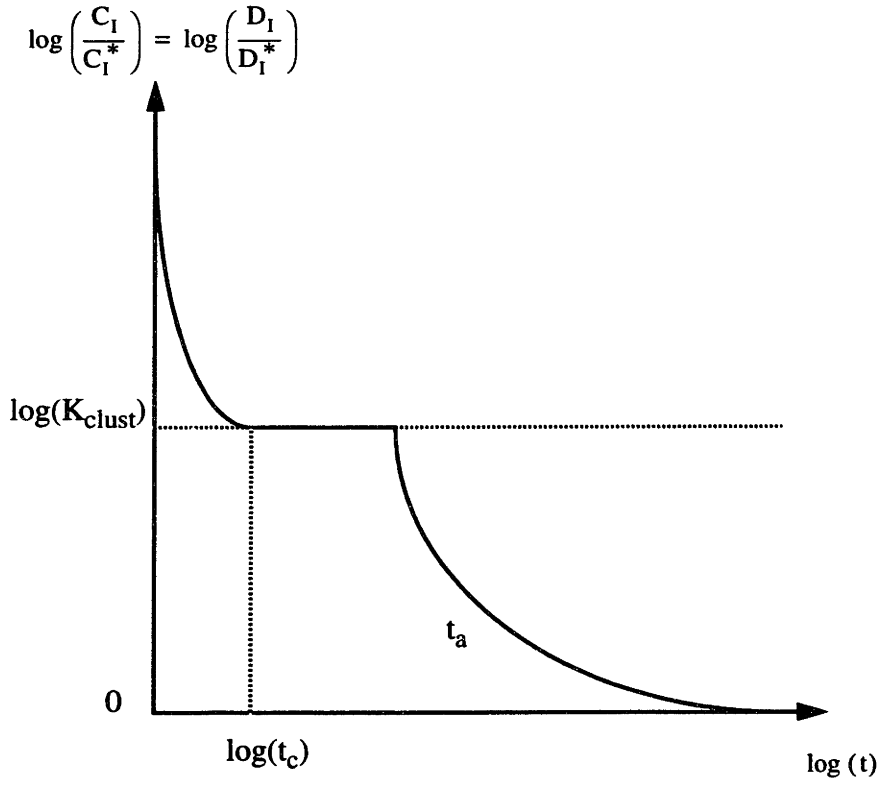

Figure 2.5: Schematic showing the time evolution of normalized interstitial supersaturation and hence normalized boron diffusivity.

A plot of the normalized interstitial supersaturation vs. time for the +f model is shown in figure 2.5. The figure shows that for short times, there should be a large initial interstitial supersaturation as the clusters are being formed, which will cause large initial boron

diffusivities. However depending on the time to form the clusters t_c, this large initial spurt of boron diffusion, given by equation (2.3), may or may not be measurable. Once the interstitial clusters have reached equilibrium, the interstitial supersaturation will, to a first approximation, be constant until the clusters are unable to support this maximum level of supersaturation. The interstitial supersaturation should then decay away with some characteristic time constant, t_a.

Finally, in this report, the initial distribution of the interstitials is assumed to have the same distribution as those of implanted ions. Thus the parameter, f, will also contain a correction factor if the initial distribution is not the same as the implanted species.

2.5 Summary

In section 2.3, several important parameters of the TED model were highlighted. Unfortunately, several of these parameters have not been measured very accurately or in some cases have not been determined. For example, up to this point in time, the importance of K_{surf} on bulk diffusion has not been determined. Similarly a value for K_{clust} should be measured using time evolution experiments. Another important parameter in the TED model is D_I. Although this parameter has been measured previously, there is still some variance in the interstitial diffusivity in the literature [22-24]. One of the objectives of the experiments presented in chapters three and four will be to determine values for the above mentioned parameters.

Chapter 3

Effect of Implant Damage on Stabilized Boron Marker Layers

3.1 Overview

Isothermal anneals after low dose silicon ion implants were studied by Packan [14]. The implant damage was introduced above a stabilized boron marker layer and the diffusion of the marker layer was studied. The experiment showed that the effect of TED occurs for times on the order 10-100 minutes, if the anneal temperature is between 800°C and 850°C. Packan's anneal times were relatively long, on the order of tens of minutes since these times were required to give him measurable diffusion lengths.

Packan's experiments yielded several interesting results which have not been well explained. One important result was that the experiment showed that for low dose 80keV silicon implants (i.e. 10^{12} cm^{-2}- $10^{13}cm^{-2}$), the measured diffusion length of boron was 400 Å. The boron diffusion lengths are independent of dose at these low doses, which is surprising since one would expect that, the larger the dose, the larger the transient diffusion. Furthermore, Packan's data and similar isothermal experiments done by Angelucci et. al. [36] seem to indicate that the enhanced diffusivity is constant during the course of annealing. These findings are also surprising since one might expect the diffusivity to monotonically decrease as damage is annealed.

3.2 Experimental Procedure

3.2.1 Sample preparation

Boron doped marker layers were grown on five inch wafers using rapid thermal CVD. Two boron doped layers of areal density $4x10^{12}cm^{-2}$ separated by a 4000Å buffer layer were deposited on a bare silicon wafer. A buffer layer of 4000Å of undoped silicon was also deposited above the shallower marker layer, while the second marker layer was in contact with the silicon substrate.

Due to the high growth temperature of 1100°C, the boron layers broadened significantly during growth, resulting in 2 Gaussian shaped boron layers at depths 4000Å and 8000Å below the surface of the silicon. The layers had peak concentrations of $5x10^{17}cm^{-3}$ and full width half maximums of approximately 1000 Å. See figure 3.3. Thus the markers are intrinsically doped for diffusion at 800°C which removes any concern for electric field or fermi level effects.

The doped layer which was closer to the surface served as the primary marker layer with which boron diffusion was measured and will be referred to as Marker I. The other doped layer was used to measure the diffusion length of interstitials in the CVD grown material and will be referred to as Marker II.

The experiments were carried out in the following order:

3.2.2 Control experiment to study RTA of small pieces

In order to heat small samples in the Rapid Thermal Anneal (RTA) system, a sample holder as shown in figure 3.1 was needed to hold the samples. The sample holder was a 5 inch wafer, with a large depression labelled A formed by etching the silicon to a depth of 300 microns. This depression acts as a "holder" for a small piece. A sample holder is nec-

essary because the RTA machine can only handle full 5" wafers, while the samples which will be annealed are much smaller.

The purpose of this experiment is to calibrate the temperature that the small sample attains during the course RTA. This control experiment is important because the system is run in close loop. The temperature of the back side of the sample holder, measured by means of an optical pyrometer, is fed back to the control electronics of the RTA machine enabling the oven to maintain a steady temperature. Thus, if the sample is not in good thermal contact with the sample holder, the sample will not be annealed at the correct temperature.

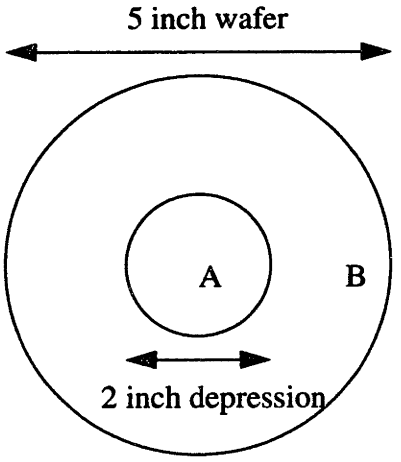

Figure 3.1: Schematic of wafer "holder" used for the RTA of small samples

In this experiment, a small piece of silicon, which had received a $2x10^{14}cm^{-2}$, 40 keV B implant was annealed in the RTA, by placing it on a sample holder which had received the same implant. The thermal budget of the anneal was 1000°C for 1 min followed by 1000°C for 5 min in an Ar ambient. Another small piece of silicon, which received the above mentioned implant, received just the 1 min 1000°C anneal. The first 1 minute

anneal was designed to remove TED effects, so that the diffusivities extracted from the subsequent 5 min can be compared to literature values. These samples are then profiled using SIMS and the resulting diffusivity extracted.

3.2.3 Short time evolution experiment

The boron doped marker layer samples received implants of $5x10^{13}cm^{-2}$ silicon ions at 80 keV and anneals at 800°C for various times ranging from 5 sec to 40 min. The implants were designed so that the maximum damage depth is about 2000 Å and the temperature was chosen to maximize the amount of diffusion, whilst allowing for a reasonable amount of diffusion in a short period of time.

The emphasis of this experiment is on the time evolution of the diffusion coefficient for times which were much shorter than those used in a similar experiment by Packan. Short time diffusivities are essential in understanding the mechanism of TED, in particular to determine if the supersaturation of interstitials is the same at short times as at long times. See figure 2.5.

3.2.4 Variation of TED with dose

The above experiment was repeated at doses of $1x10^{12}cm^{-2}$ and $1x10^{13}cm^{-2}$ with the lighter dose being repeated at energies of 25 and 40 keV. The experiments are meant to examine the dependence of TED with dose and energy, especially under low energy, low dose conditions, which Packan did not do. These implant conditions are important because they are used frequently in Lightly Doped Drain (LDD) implants. Low dose implants produce a lot more transient diffusion than would be expected from a simple linear dependence of damage upon implant dose. The dependence of TED on implant dose was found in [14] to be surprisingly weak. It is important to characterize this low dose limit as it sug-

gests that even low implant doses can cause TED effects which are readily measurable in devices as is the case in [3]. In addition, it is well known that at low energies, TED effects diminish rapidly with decreasing implant energy [14, 24 & 38].

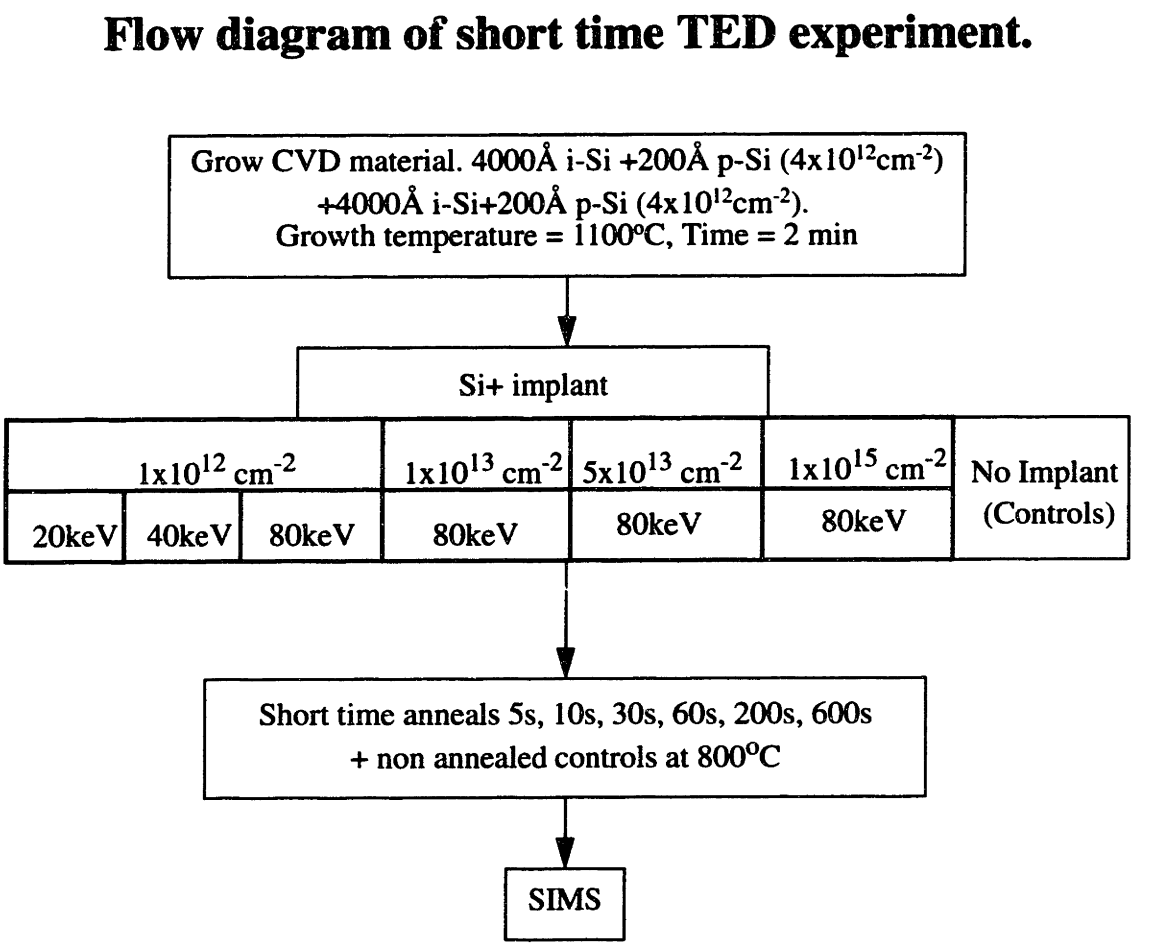

Figure 3.2: Flow diagram of short time TED experiment.

3.2.5 Procedure to extract the diffusion length of boron

In order to extract the diffusion length of boron, SIMS analysis was performed on all the samples to obtain boron profiles before and after the anneals. The initial and annealed boron profiles were then analyzed at each anneal time to extract the diffusivity of the

boron and the magnitude of the profile shift. The analysis method was a two parameter least squares fit performed by computer program since a manual calculation for a fit to a SIMS profiles, which has hundreds of data points would be exceedingly tedious. Each of the two markers were analyzed separately so that diffusivities for both marker layers could be extracted independently. The minimum detectable diffusion for Marker I can estimated from considering the signal to noise ratio (15 dB) of the SIMS data and was estimated to be about 10 nm. The corresponding number for Marker II is estimated at about 15 nm. Although the SIMS depth accuracy is about 5 nm, the extraction of diffusivity is an average over hundreds of points so the degree of freedom in the fit is large. The error in the diffusion length of boron in Marker I for diffusion lengths of more than 20 nm, can be conservatively estimated at 30 nm while that of Marker II was set at 50 nm. For difusions lengths of less than 20 nm, the error was set arbitrarily at about 10 nm, indicating that some diffusion must have taken place although the exact magnitude is not known with a great deal of certainty.

3.3 Results and Discussion

3.3.1 Control experiment to study RTA of small pieces

The results of the control experiment were excellent. The boron profile of the sample was the same as in the holder and were in agreement with the literature value. The boron diffusivity in the small sample was within the error of the SIMS profiling technique and shows agreement with the literature value at 1000°C or about $1.5 \times 10^{-14} cm^2 s^{-1}$. Thus, the pyrometer reading of the RTA was well calibrated to the annealing temperature of the samples on the sample holder wafer.

3.3.2 Short time evolution experiment

Dose dependence

The samples which received low dose implants i.e. $1x10^{13}$ cm^{-2} or less, exhibited no measurable TED (less than 20nm compared to Packan's value of 40 nm). In addition, the samples which received the $1x10^{15}$ cm^{-2} and $5x10^{13}cm^{-2}$ implants exhibited maximum diffusion lengths of about 45 nm (see figure 3.5) vs. Packan's published value 75 nm.

The above 2 points are consistent with less TED in the CVD grown samples with respect to Packan's data. There are several reasons why this may be the case:

• The CVD grown material has a large number of vacancies or traps which reduces the number of available interstitials which may take part in diffusion. This model does not give good fits to the measured data if the traps are assumed to be uniformly distributed throughout the material. However, if one assumes that the elevated growth temperature resulted in the dynamic annealing of damage as the sample was grown, this could have left a vacancy rich or trap filled region near the surface, but close to the implant.

• The D_IC_I product in CVD material is more than in float zone material, used by Packan. There is some evidence that material preparation can significantly affect the interstitial diffusivity and D_IC_I. For example, MBE material shows significantly less OED than float zone (FZ) or Czochralski (CZ) material [22]. If the material is "cleaner" than FZ or CZ material, then it is possible that $(D_IC_I^*)_{CVD}>(D_IC_I^*)_{FZ}$. However, there is small scatter in the literature in D_IC_I in silicon so this explanation is not very satisfactory and more experiments must be done to check this hypothesis.

• Boron may be clustering in CVD grown samples, since the peak boron concentration in the CVD grown samples is an order magnitude higher than the peak of Packan's samples. The problem with this explanation is that the shape of the boron concentration profiles look extremely gaussian and even at low concentration, diffusion is not observed.

Another interesting point is that the diffusion length of boron in the $1x10^{15}$ cm^{-2} Si^{+} implanted samples same as those of $5x10^{13}$ cm^{-2} samples for the short anneal times of less than 60s and the longest anneal time of 40 minutes. For times between 60 s and 10 minutes, the higher dose implant caused significantly less transient diffusion than the lower dose implant. This difference in the diffusion length is most pronounced after the 200 s anneal.

One reason for the difference between the two implants is that the $1x10^{15}cm^{-2}$ silicon implant is amorphising. Thus a large quantity of interstitials are trapped in end-of-range (EOR) dislocations and are released slowly on annealing. Since the time constant for annealing of these dislocations is much more than 40 minutes most of the interstitials which are trapped in these loops will not contribute to TED of boron. In fact, the 40 min anneal of the $1x10^{15}$ cm^{-2} Si^{+} implanted sample shows that some of the boron is segregating into the region EOR damage as shown in figure 3.4.

In fact, it is more surprising that the high dose $1x10^{15}$ cm^{-2} Si^{+} implant showed similar annealing characteristics as the $5x10^{13}cm^{-2}$ Si^{+} implant. Despite the great difference in the initial damage levels and damage distribution, the boron diffusion lengths in the first minute of annealing, were not significantly different.

Time evolution of diffusivity

Figure 3.5 shows that the diffusion length of boron due to the silicon damage implants increases rapidly for the first minute of annealing. However, the diffusion length of boron saturates after ten minutes for a damage dose of $5x10^{-13}cm^{-2}$.

The diffusivity D_B saturates at 6000 x D_{inert} for times shorter than 60 s and rolls off for times of more than 60 s. This results suggest a maximum enhancement term, K_{clust} (see section 2.4), of about 6000, which means that when the concentration of interstitials

reaches about 6000 times the intrinsic interstitial concentration, C_I^*, the interstitials cluster. This result is qualitatively in agreement with previous work done by Giles [8] on phosphorous and Packan [14] in silicon as shown in figure 3.6. A larger maximum enhancement of about 10^4 is seen by Giles and could be due to the different material quality between his epitaxially grown material and the CVD grown material.

The clustering model could also explain why damage annealing in times of less than 1 minute between both the low and high dose implants were so similar In the first minute of diffusion, the concentration of the clusters in the heavily damaged regions is so large that the rate of release of interstitials from the clusters will be diffusion limited in both samples. Thus, the total amount of interstitials reaching the boron markers is the same in the two samples. At times of more than 60 seconds, the more stable end of range dislocations form when these clusters coalesce and compete with the dissolution mechanism. Thus fewer interstitials are available for TED in the samples which received a higher silicon dose.

The damage distribution model, proposed in chapter two implies that may be a very large initial diffusivity at the outset of diffusion before the interstitials begin to cluster. However, the short anneal times of 30 s or less indicate that if there is a large initial enhancement of say 10^5 times normal, it would have to occur in times of less than five seconds. The starting profiles were too broad in this experiment to measure diffusion at 5 s.

In summary, the profiles diffused with an approximately constant diffusivity of 6000 times more than that in thermal equilibrium, for both high and low dose damage. If there is an initial "hyper-transient" it must finish in a very short time and contribute little to the total diffusivity.

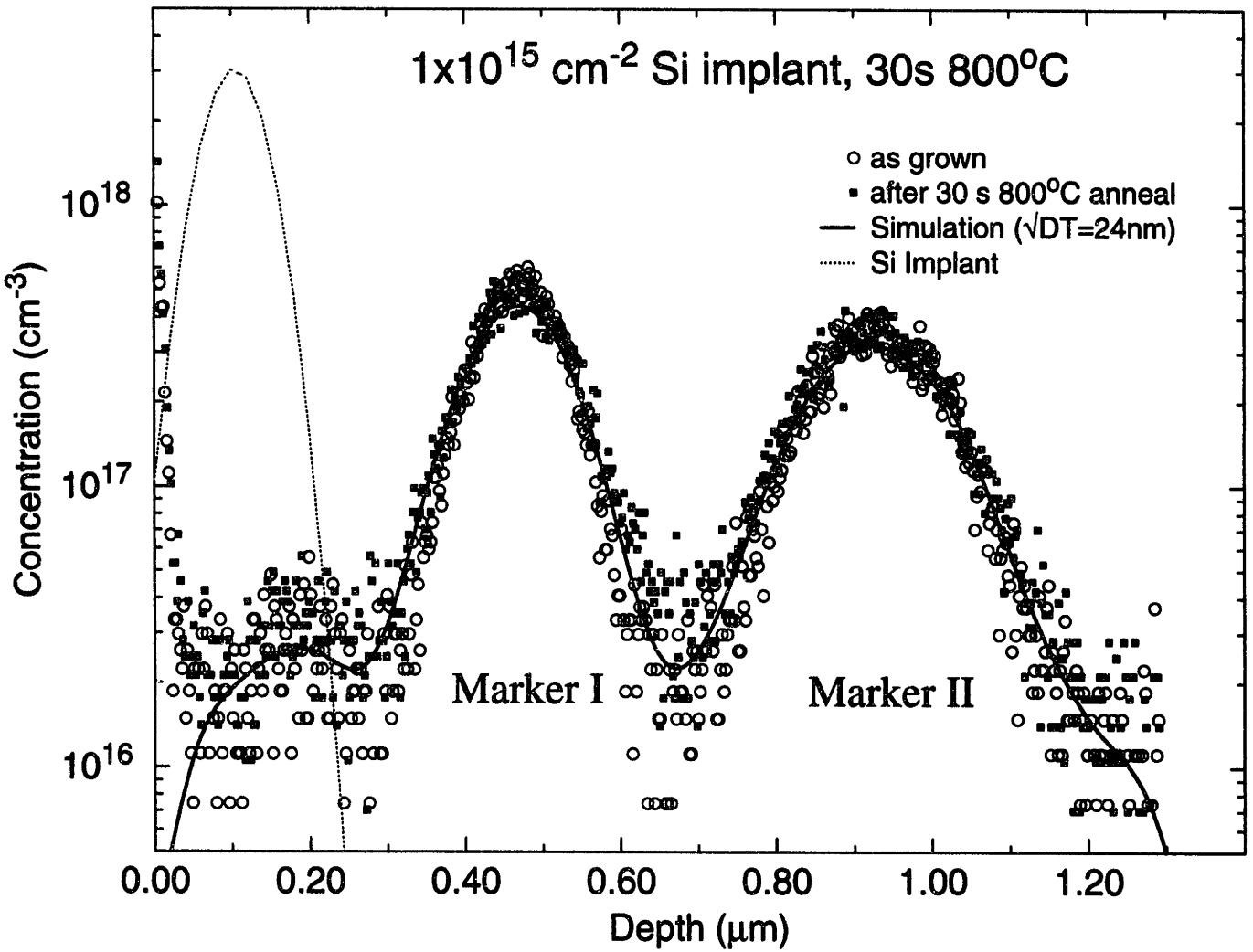

Figure 3.3: SIM results of the sample which received a Si^+ dose of $1x10^{15}$ cm^{-2} and a 30s 800°C anneal.

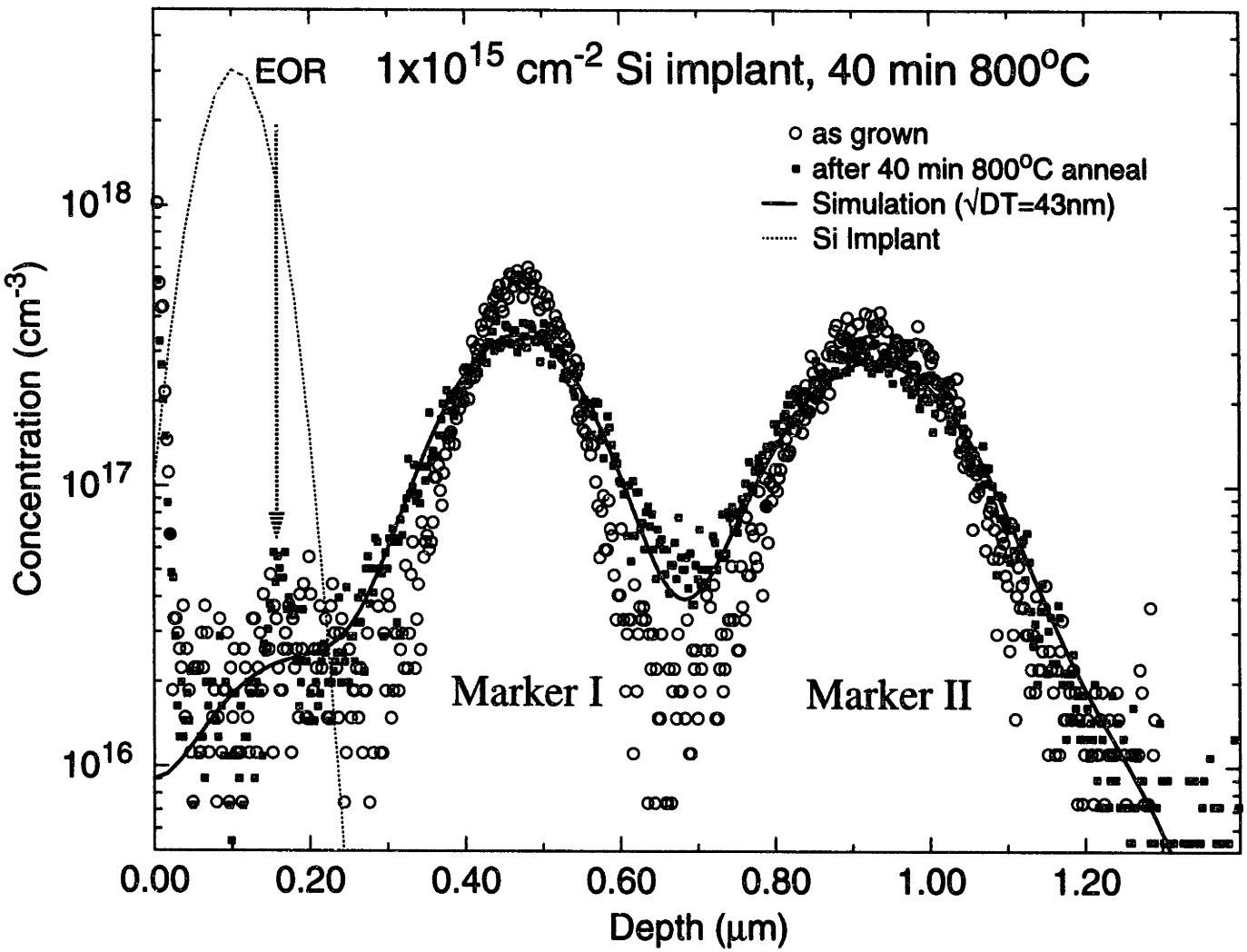

Figure 3.4: SIMS results of the sample which received a Si^+ dose of $1x10^{15}$ cm^{-2} and a 40 min 800°C anneal.

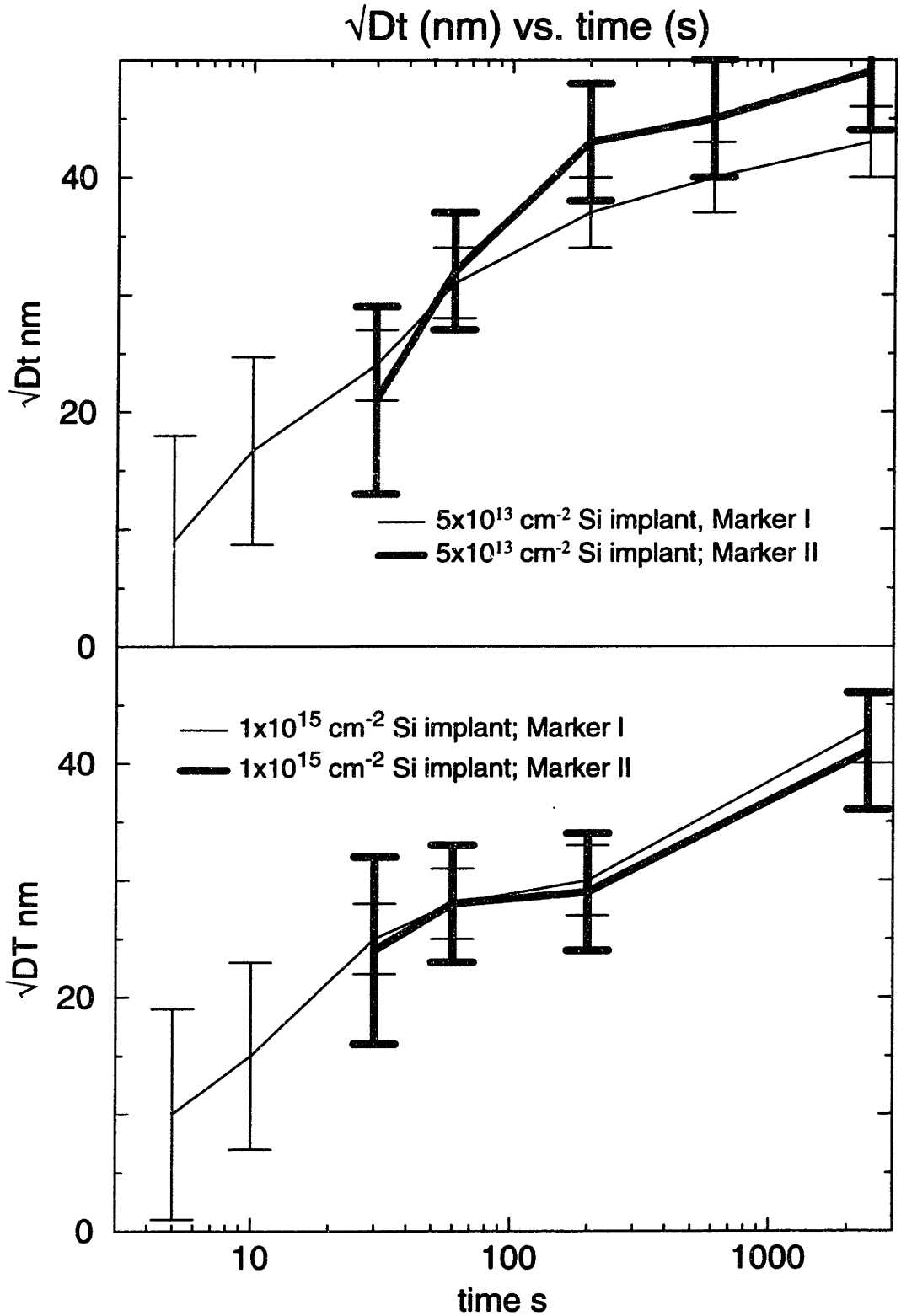

Figure 3.5: Plot of diffusion length vs. time

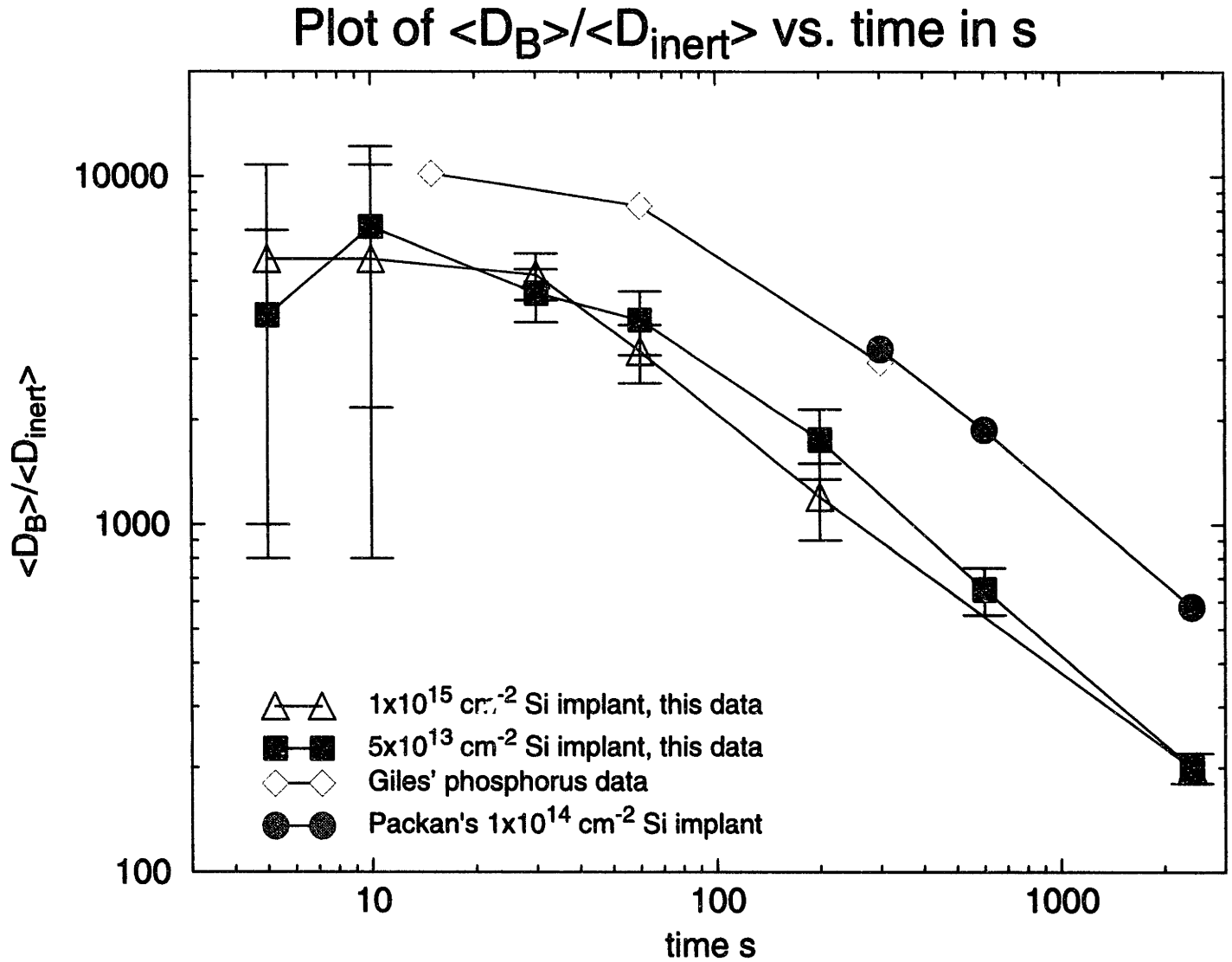

Figure 3.6: Plot of normalized time averaged diffusivity vs. time in s

Diffusion length of interstitials

Figure 3.5 also shows that the diffusion length of boron extracted from Marker I is, within error, the same as the diffusion length of boron extracted from Marker II for all times more than 30s. Since the interstitials have moved from 0.1 μm to 1 μm in less than 30 s, the diffusion length of the interstitials must be greater than one micron in 30s. Thus, the interstitial diffusivity D_I may be estimated from $\sqrt{D_I t} > 2*1$ μm, i.e. D_I is on the order of $10^{-9} cm^2 s^{-1}$.

"Time of flight" diffusivity refers to a method of measuring and extracting the interstitial diffusivity by studying how long it takes for interstitials to travel from the point of damage to some distance away from the damage to broaden a marker layer profile. Time of flight measurements are the most direct way of measuring interstitial diffusivity and hence are valuable for modeling TED.

Figure 3.7 shows several estimates of the time of flight interstitial diffusivity in the literature. Although the estimate of the time of flight interstitial diffusivity is more than a factor of 3 larger than previous estimates at 800°C, the extracted interstitial diffusivity from this experiment agrees well with previous results by Bronner et. al. [23] and Griffin et. al. [24]. The interstitial diffusivity data from Bronner et. al. were calculated directly from their experimental results using time-of-flight arguments rather than from their analysis. The reason for this is that their analysis required several assumptions which may not be true, such as the assumption that the total amount of damage released during anneal is independent of temperature

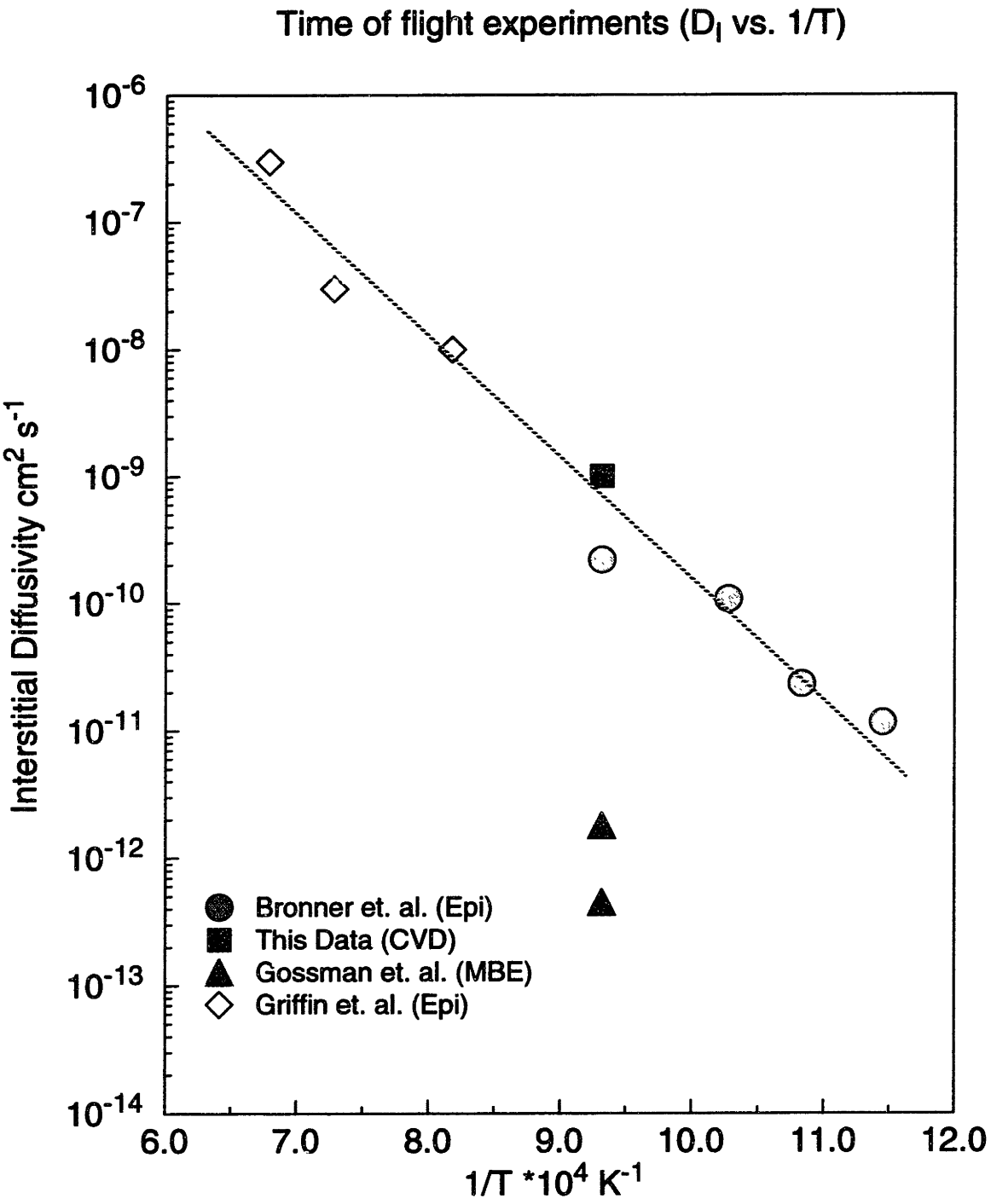

Figure 3.7: Time of Flight Experiment Results

Modeling of Short time experiment

The long time it takes to anneal out the transient (on the order of tens of minutes) and the short time it takes for the interstitials to reach the second marker layer indicates that a good model for TED requires a combination of high interstitial diffusivity and clustering of the interstitials. Thus in order to model the short time experiment, I used the two parameters extracted above, i.e. $D_I = 1x10^{-9}\ cm^2\ s^{-1}$ and $K_{clust}= 6000$ and simulated TED using the point defect model in PROPHET. A value of $D_IC_I^* \sim 500\ cm^{-1}s^{-1}$, which is consistent with the value in literature ([25] and [26]), and a large value for K_{surf} of 1 μm/s was also used in the simulations. The assumption of fast surface recombination was examined, and supported, by the surface experiments described in the next chapter.

In order to model transient diffusion, PROPHET solves the point defect model on a grid. As was mentioned in chapter two, this model consists of a system of coupled differential equations which describe point defect diffusion and the interaction of point defects with boron. Thus, in this model an impurity profile (boron in this case) and a point defect profile are required as initial conditions. The initial impurity profile used in modeling this experiment is the as grown boron profile shown in figure 3.3 while the point defect distribution was determined from standard implant tables [27]. The areal density of the distribution was normalized to the product of the implant dose and f. A value of f=0.3 was found to cause a reasonable amount of transient diffusion, 45 nm, in a time of 40 minutes.

Figures 3.8 and 3.9 show that values, $D_I = 1x10^{-9}\ cm^2\ s^{-1}$ and $K_{clust}= 6000$, provide good fits to the diffusion vs. time data. However, the simulations with $D_I=10^{-10}cm^2\ s^{-1}$ and $K_{clust}=0$ show that the diffusion of Marker I proceeding too rapidly, although the time evolution fit to Marker II is excellent.

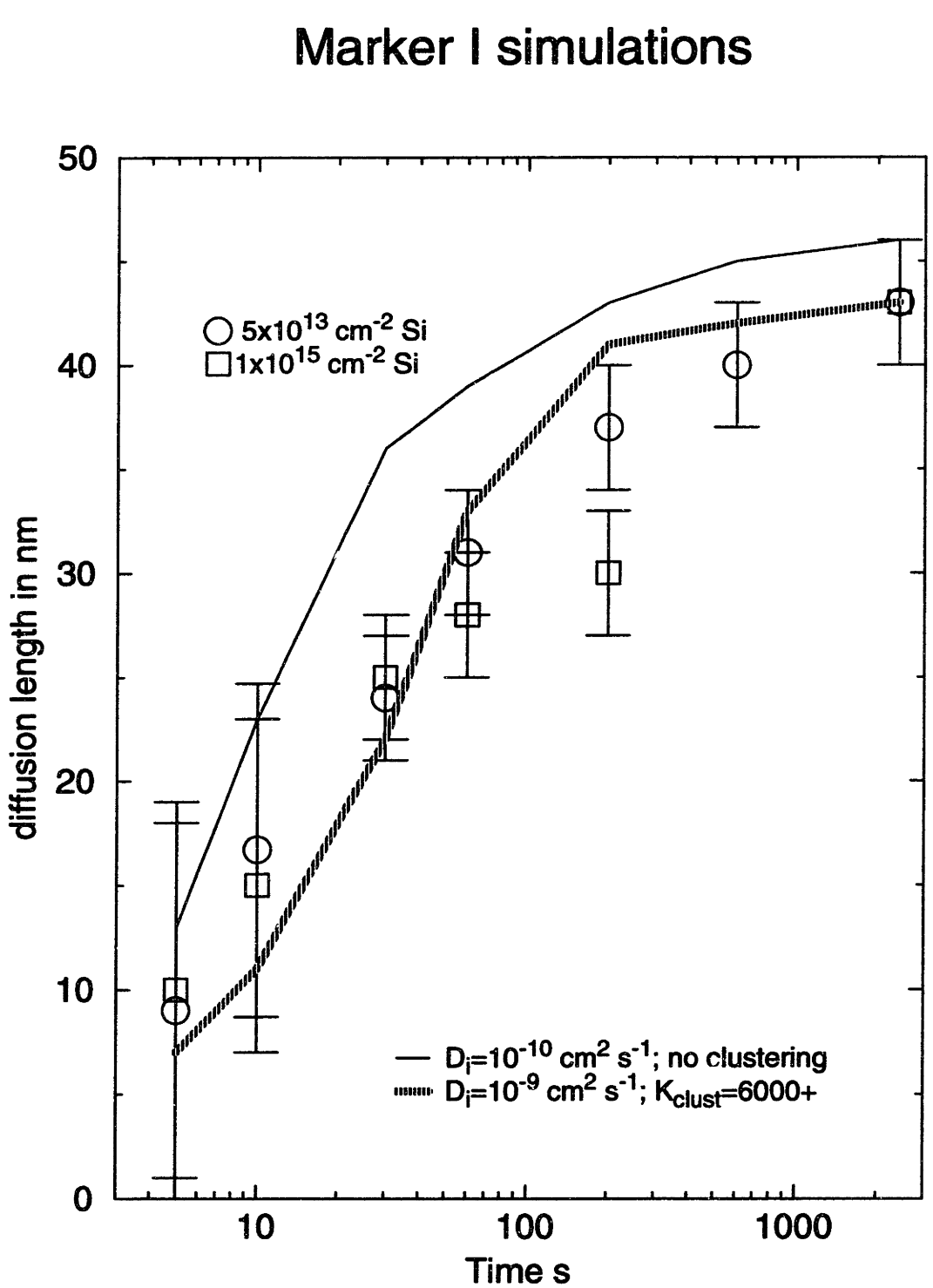

Figure 3.8: Simulations to fit the time evolution of diffusion Marker I.

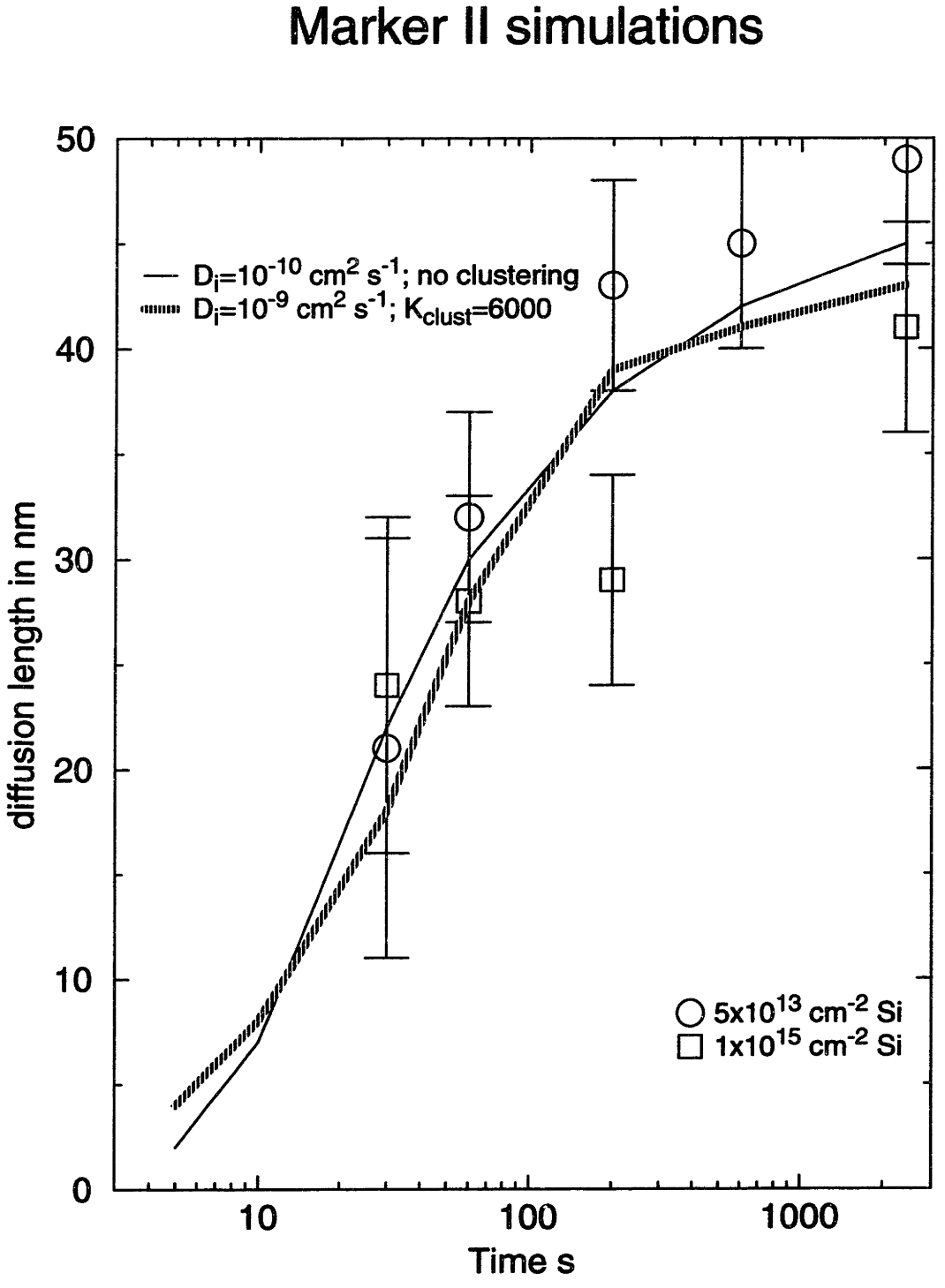

Figure 3.9: Simulations to fit the time evolution of diffusion Marker II.

Chapter 4

Effect of Surface Proximity on Transient Enhanced Diffusion

4.1 Overview

Several authors have shown that the magnitude of transient enhanced diffusion increases with increasing implant energy until about 80 keV [14, 24 & 38]. There are two schools of thought as to why TED increases with energy. The first is that higher implant energy causes more damage which in turn causes more enhanced diffusion. The second is that the surface acts as a strong recombination sink for interstitials which greatly reduces the effect of TED. The closer the surface, the more effective the sink. Although it may seem obvious that the surface should be a strong sink for interstitials and vacancies, many experiments thus far indicate otherwise.

Griffin et. al. [24] showed that for the same implant energy, boron, phosphorus and arsenic implants caused similar amounts of TED of a boron marker layer. This result might suggest that the surface recombination is unimportant since the implant range of arsenic is about a factor of five less than that of boron.

Gannin et. al. [30] showed that the surface had little effect in the formation and anneal kinetics of dislocation loops in EOR damage. Furthermore, Narayan et. al. showed that annihilation of near surface dislocation loops is due largely to the gliding of the loops to the surface [31], implying that the dissolution of the loops and the subsequent diffusion of interstitials to the surface was a small effect.

On the other hand, some experiments have shown that annealing is strongly dependent on surface effects. Kim et. al. showed that when the near surface region of an amorphising

BF_2 implant was etched, TED was virtually suppressed [29]. However, this experiment is not conclusive since most of the implant damage is etched away at the same time as bringing the surface closer to the damage.

The aim of the experiment is thus to determine if the surface is a strong recombination sink by varying the position of the surface with respect to the damage and annealing out the transient.

4.2 Experimental Procedure

The main difficulty in this experiment was that in order to make the experiment conclusive, the effect of damage being etched away had to be de-coupled from the effect of moving the surface closer to the damage. The only way to achieve this is to use a high energy silicon implant over an even deeper stabilized boron marker layer. The dose of the silicon implant was chosen so that extended defects, if formed, would anneal out in a reasonable amount of time, while the dose of boron was chosen so that diffusion would be intrinsic at 800°C.

$1x10^{13}$ cm^{-2} of B^+ was implanted at an energy of 200 keV into 10-20 Ω cm p-type silicon. This implant was followed by an anneal at 1000°C for one minute to remove the damage due to the boron implant. Si^+ was then implanted with a dose of $2.7x10^{13}$ cm^{-3} and an energy of 180 keV.

After the silicon implant, the wafer was cleaned and 1 μm of TEOS was deposited at a temperature of 425°C using a plasma enhanced CVD process. The TEOS would serve as a hard mask to the Reactive Ion Etch (RIE) of silicon in the subsequent step. The TEOS was then patterned as shown in figure 4.1 and Cl_2 RIE was performed in the windows to etch back the silicon to depths of 650 Å, 1000 Å, 1250 Å, 1750 Å and 2600 Å. The reason why

windows were used instead of a blanket etch was to ensure that the depth of the etch could be calibrated and measured.

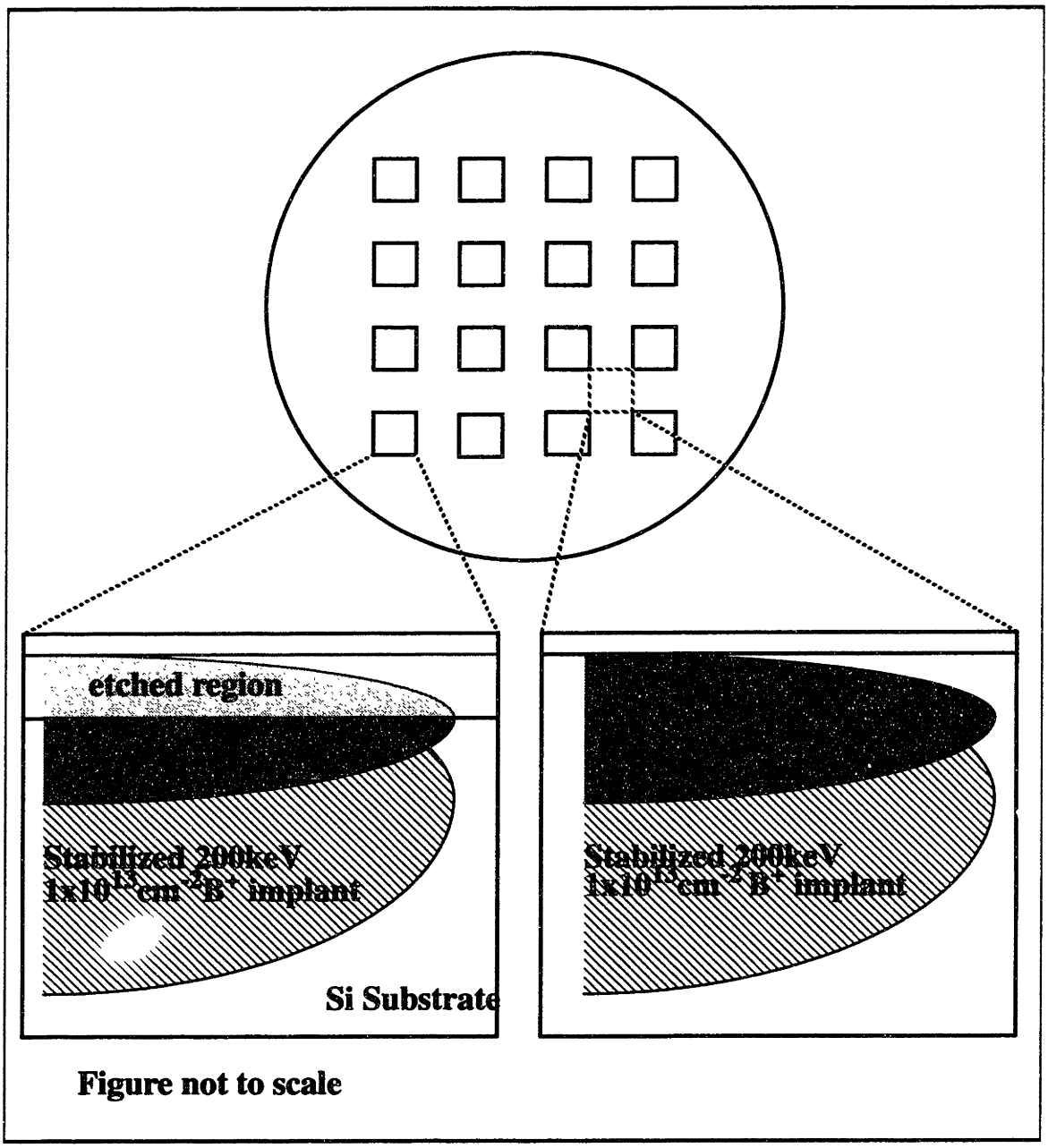

Figure 4.1: Schematic of etch back experiment.

At this point the TEOS was stripped in HF to ensure that the surface of both the etched and unetched regions of the wafer were similar. The samples were then cleaned and annealed at a temperature of 800°C for 2 hours. This anneal should completely anneal the implant damage to completion since the dose of the implant was low. The boron profiles were obtained using SIMS analysis. Several controls are included in the experiment -- there were two unetched unannealed samples and one unetched annealed sample.

4.3 Results

Calibration of Etch Depth

The depth of the etch was calibrated carefully as this quantity would determine the proximity of the surface to the damage. In fact, the etch depth of each samples was determined using three separate techniques. The first technique was to measure the total oxide/silicon step immediately after the RIE. By measuring the depth of the oxide/silicon step using a profilometer, it is possible to ascertain the amount of silicon etched off, if the TEOS thickness is known.

The etch depths were also determined after the oxide etch. In this case, the profilometer measured the step directly and the etch depths were within 100Å of that determined immediately after RIE. The roughness at the bottom of the window, as measured by the profilometer, was less than 100Å peak to peak, over a profile over 2 mm long. The third technique of determining the etch depth was to align the peaks of the boron SIMS profiles. All three techniques yielded similar values for the etched depth of each sample.

Effect of RIE

The roughness at the bottom of the etched window due to the RIE might have caused problems in the SIMS analysis. The surface roughness of 100Å would result in an appar-

ent broadening of the boron profile since the resulting SIMS profile would be a convolution of the surface roughness with the actual profile. However, the surface roughness was shown to have a negligible effect on the resulting boron profile. This conclusion can be drawn from the observation that there was no visible difference in the annealed profiles between the unetched and the sample etched by 650Å. See figure 4.2.

More importantly, this implies that the RIE etch itself did not increase or decrease significantly the amount of damage in the near surface region. Automatic diffusion length extractions showed that the latter boron profile exhibited less TED, confirming the visual impression that RIE caused no extra TED.

Errors in the diffusion length

In the previous chapter, the method of extraction of the diffusion length of boron from a SIMS profile was explained. Again the minimum detectable diffusion of boron can estimated from signal to noise ratio (25 dB) considerations and was estimated to be less than 200 Å. In addition, the error in the diffusion length of boron for diffusion lengths of more than 200Å was estimated at 30Å.

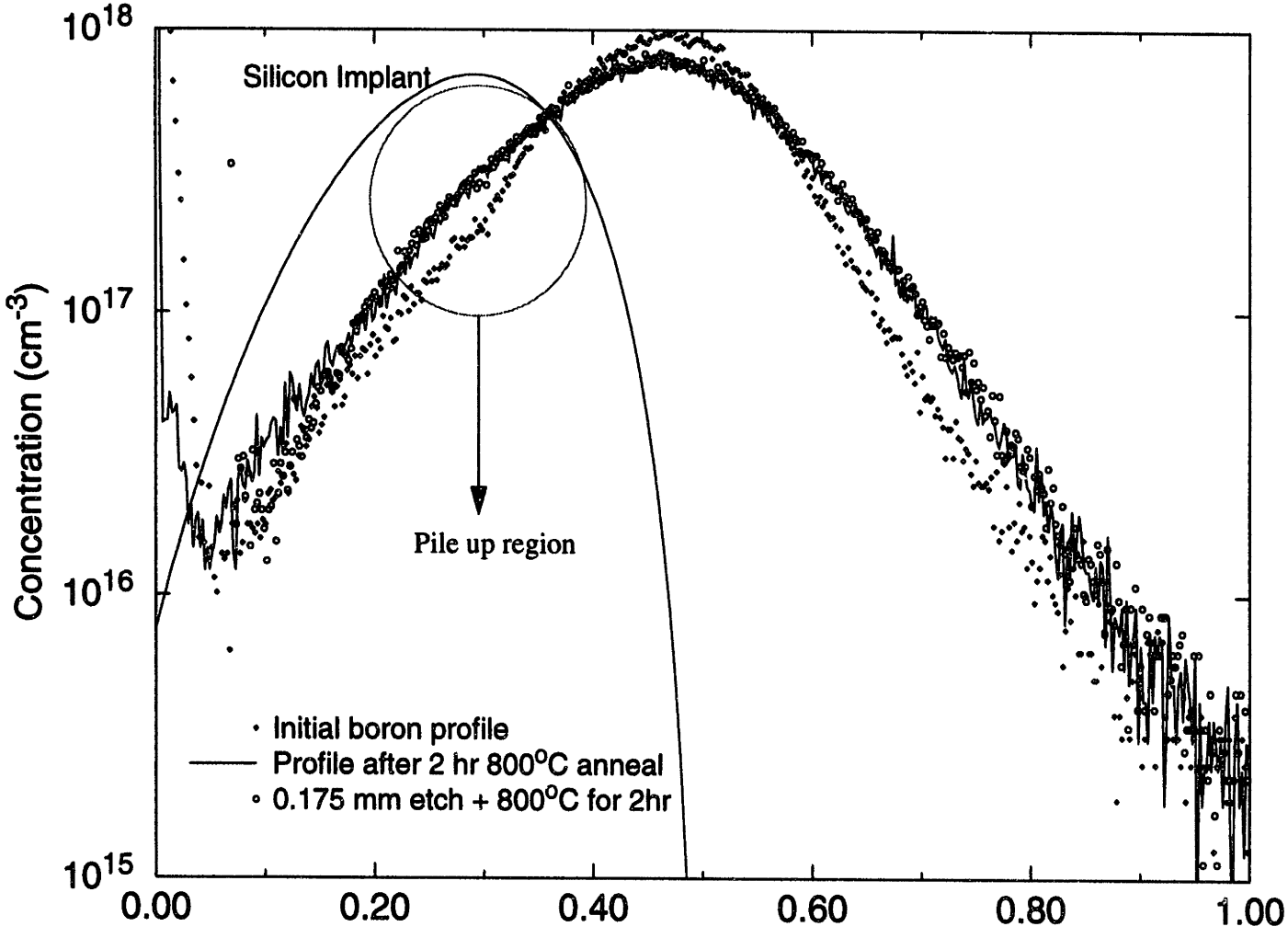

Figure 4.2: SIMS results of the unetched control and 0.065 μm etched sample

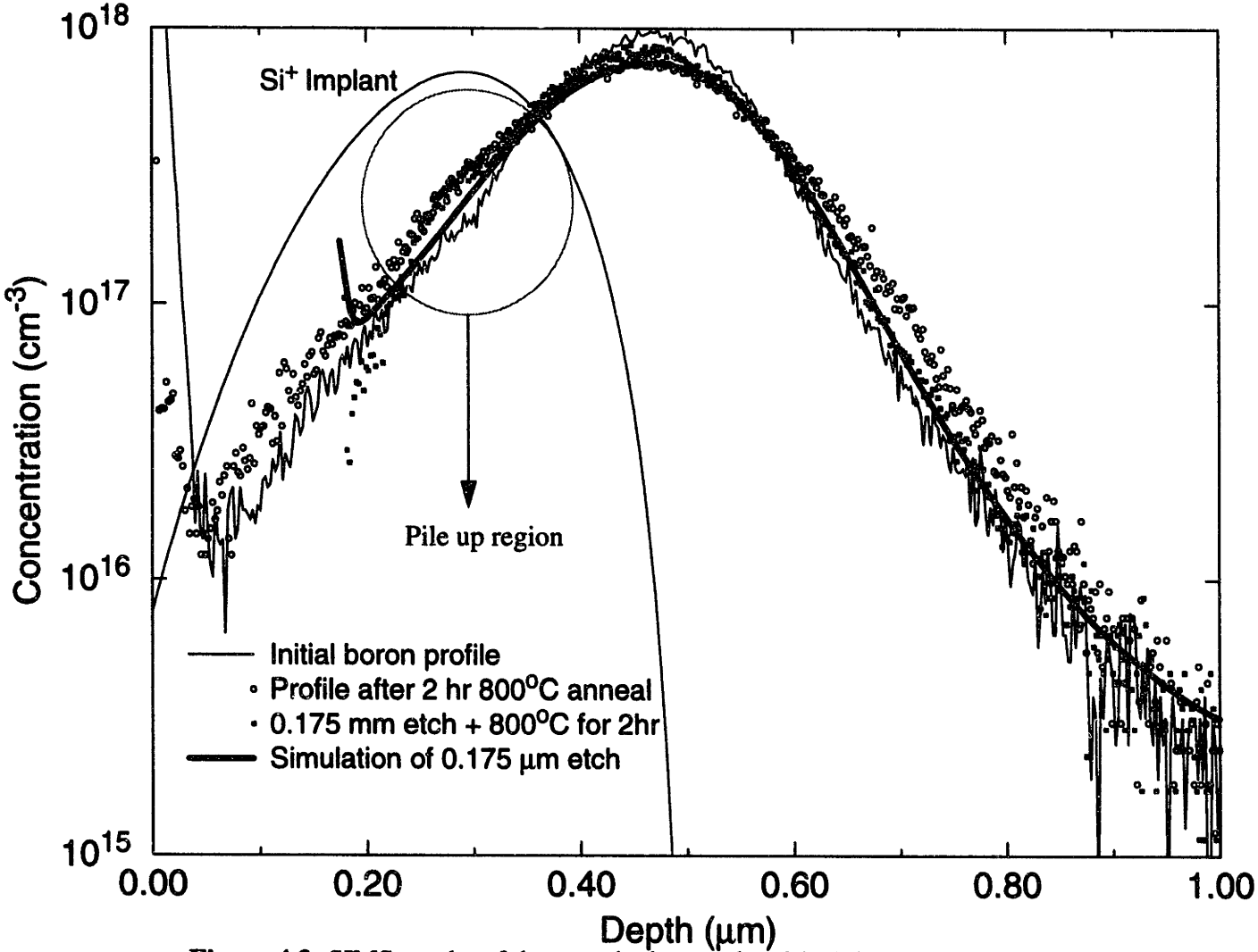

Figure 4.3: SIMS results of the unetched control and 0.175 μm etched sample

Effect of surface proximity on the diffusion length of boron

The SIMS results for the sample which was etched by 0.175 μm is shown in figure . This figure shows that there is significantly less diffusion in the etched sample compared with the unetched annealed control sample as shown in figure 4.2.

The plot of boron diffusion length $\sqrt{Dt}$ (nm) vs. etch depth (μm) of silicon is shown in figure 4.6. This figure shows that the diffusion length of boron when the etch depth is 260 nm is reduced to less than 20 nm from a value of 50 nm in the unetched control. This reduction in boron diffusion length is more than a factor of 2.5 which implies that the diffusivity of boron is reduced by more than a factor of six. From equation (2.3)

$$\langle D_B \rangle t = \int_t \frac{D_B}{D_B^*} dt \approx \int_t \frac{C_I}{C_I^*} dt$$

Thus to fully explain the reduction in the boron diffusivity, the damage and hence C_I should have been reduced by a factor six.

By using a TRIM simulation [28], the damage distribution of the silicon implant may be inferred. The result of this simulation is plotted as the dotted line in figure 4.6. By taking the integral of the implant damage under this curve from 0 to 260 nm, an estimate of the reduction of the damage by the RIE step may be obtained. This is plotted vs. etch depth in figure 4.4. This reduction in the amount of damage by the silicon implant turned out to be less than a factor of 1.7 as opposed to the factor of six required to fully explain the reduction in boron diffusivity. This discrepancy, in turn, means that the there must be some other mechanism which reduces the damage in the silicon as the silicon surface is etched. Since surface proximity to the damage is the only other variable which depends on the etch depth, the surface must be acting as a strong sink for interstitials which reduces the number of interstitials available to cause transient diffusion.

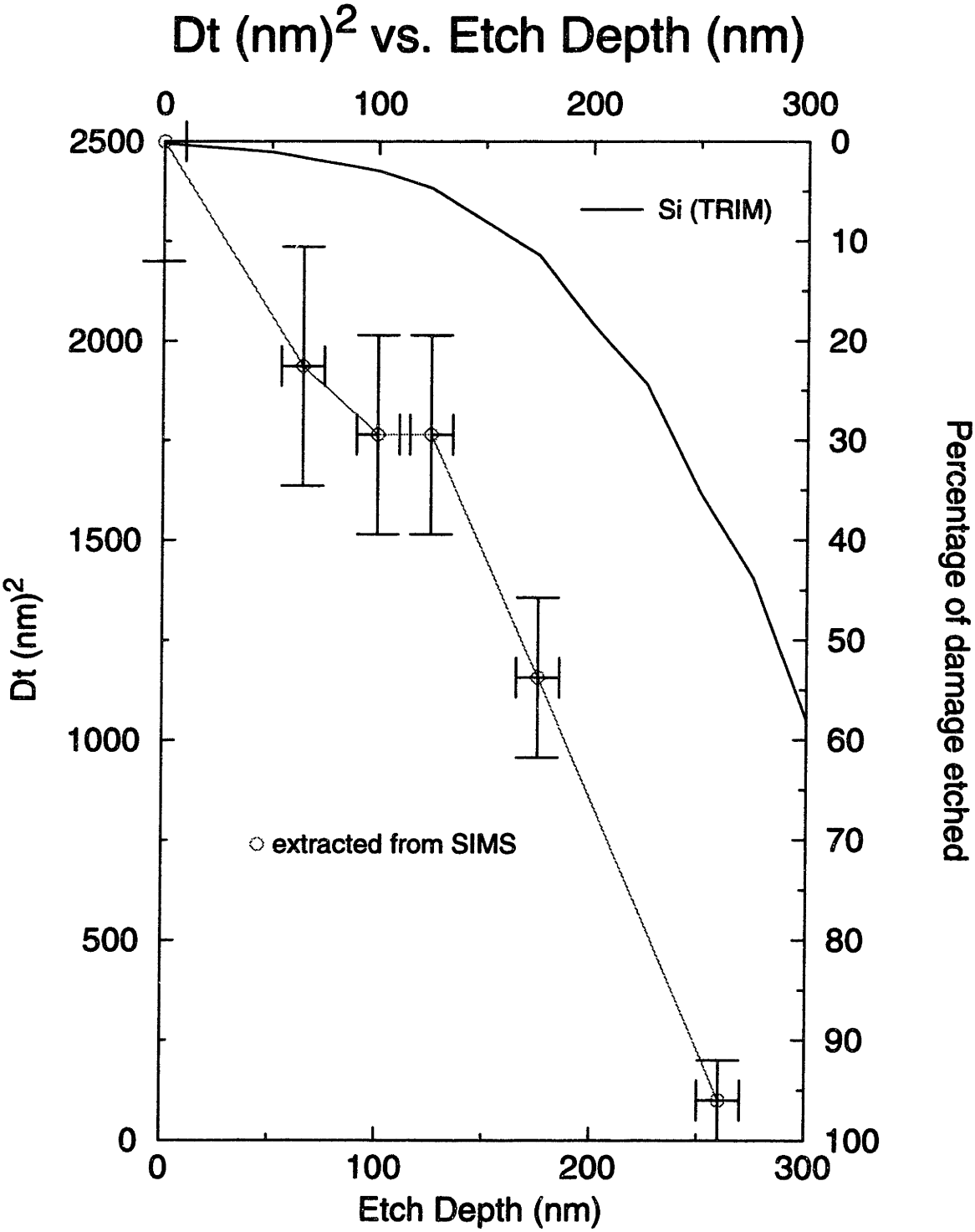

Figure 4.4: Plot of the square of the diffusion length of boron vs. percentage of damage etched away.

Pile-up of boron near the peak of the damage implant

Figure 4.2, and figure show that there exists a region close to the peak of the damage in which boron seems to "pile-up". This region of pile-up is plotted against etch depth in figure 4.5. As can be seen from this figure, the depth of the back-side of the pile-up region is independent of the depth of the etch. However, the depth of the front-side of the pile-up region decreases with etch depth. This suggests that this region of pile-up is related to a region of interstitial supersaturation and that increased proximity of the surface to this region depleted the number of interstitials.

The figure also shows that the region of pile-up is coincident with the peak of the implant damage further supporting idea that the "pile-up" is somehow related to the damage introduced by the silicon implant.

There are two possible explanations of why the boron is accumulating in that region. The first is that the large number of interstitials in the peak resulted in more enhanced diffusion near the peak ($D_{peak}>D_{average}$). Thus to maintain the flux of boron in this region of peak damage (as required by $D_{average} \cdot \nabla C_{average} = D_{peak} \cdot \nabla C_{peak}$), the concentration gradient near the peak damage is reduced. This hypothesis is supported by the fact that the concentration gradient of the boron in this region is less than the concentration gradient in the adjacent regions. A second possibility is that extended defects were formed as a result of the implant. These defects then trapped boron during the period of transient diffusion and they then trapped boron during the period of transient diffusion.

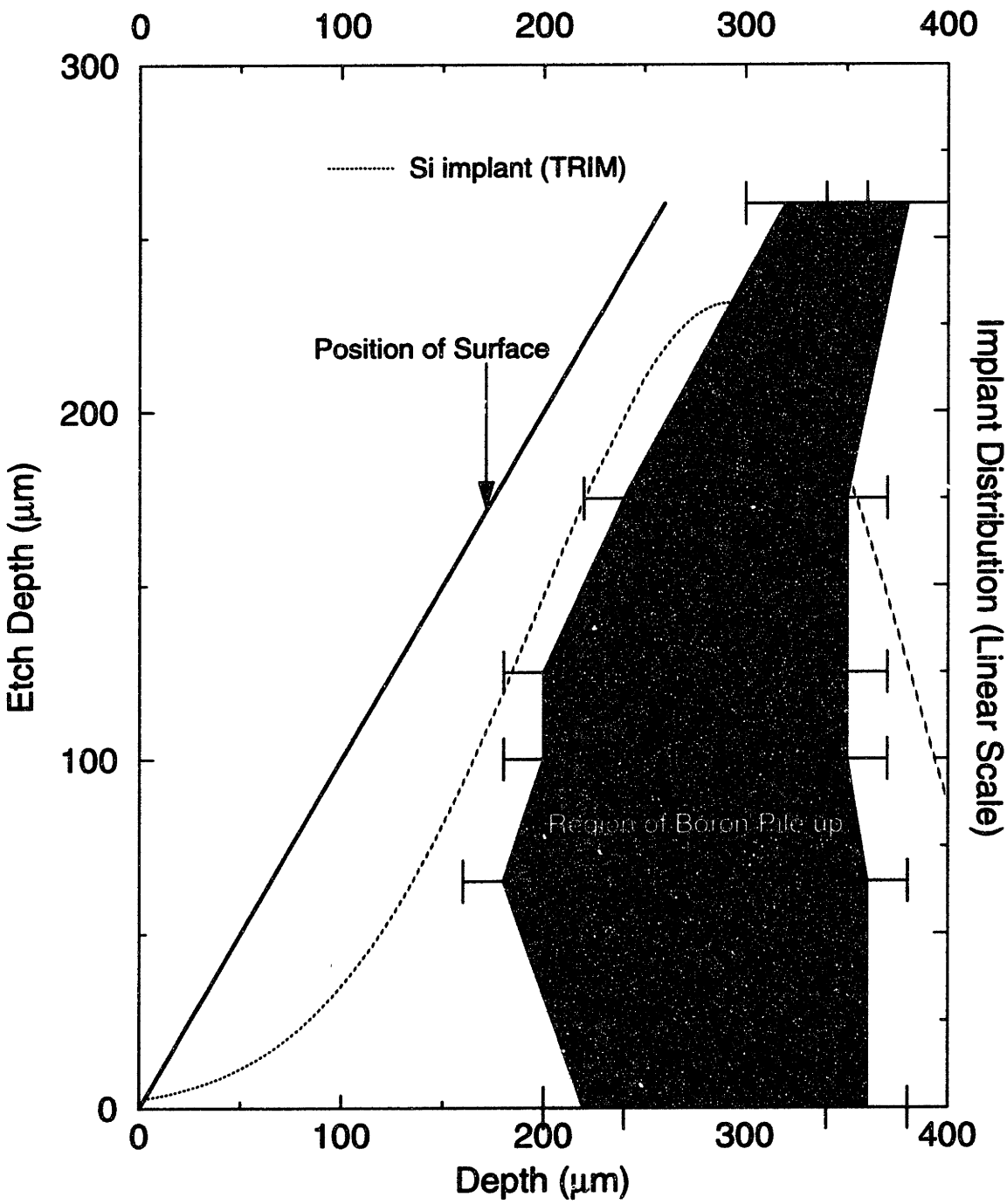

Figure 4.5: Plot of position of boron pile-up region vs. depth

Modeling of the etch back experiment

In order to model the etch experiment, the interstitial diffusivity and K_{clust} from the short time experiment in the previous chapter is used. This model provides a good fit for the data can be seen from figure 4.6.

Using a TRIM monte carlo simulation [28] to determine the distribution of the silicon implant, a simulation with a small interstitial surface recombination rate of 10^{-4} μm s^{-1} was run. A value of f=0.26 was used in the simulation, as this gave a reasonable fit to the data at shallow etch depths. The simulation is represented by the * symbols in figure 4.6 which shows that the diffusion length $\sqrt{Dt}$ is indeed reduced by a factor of 1.4 when the etch depth is 250 nm. As is apparent from the figure, this line is a poor fit to the data represented by the circle symbols. A simulation which was run on PROPHET with a large interstitial recombination rate of 1 μm s^{-1} (represented by the square symbols) provides a much better fit to the data. This result indicates very strongly that surface proximity plays an important role in the phenomenon of transient diffusion.

For these simulations, only the broadening on the deep side of the profile was used to measure diffusivity. The direct effects of damage on the shallow side such as precipitation or dislocation pile-up are not in the scope of this work.

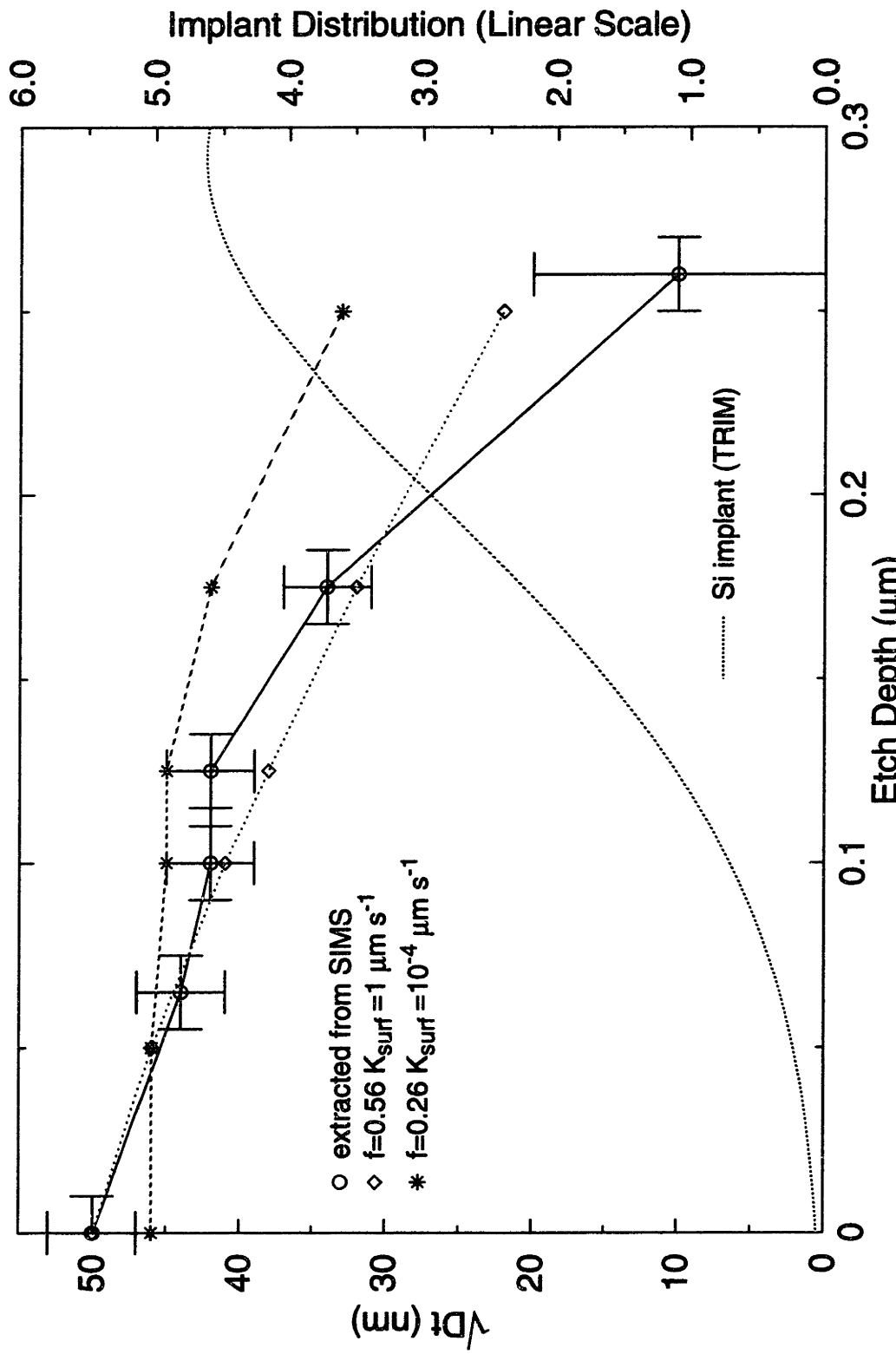

Figure 4.6: Plot of √Dt (nm) vs. Etch Depth (μm)

4.4 Discussion

In this section, the possible ramifications of the findings in this chapter will be studied. In addition, this model of strong surface recombination will be used to explain some experimental data in the literature.

This experiment shows that the effect of interstitial surface recombination must be considered when modeling TED. However, it is also important to consider that the presence of a thermal oxide or thin film at the surface could change, significantly, the surface recombination velocity.

In the beginning of this chapter, was mentioned that Griffin et. al. [24] showed that the amount of TED in a boron maker was essentially independent of the implant species. A possible reason for this apparent insensitivity to implant species is that, for the same energy, As produces much more damage than B. However, the As damage is much shallower than B damage. This experiment shows that proximity to the surface reduces the effect of TED so these two effects probably trade-off.

The reduction of TED by bringing the surface closer to or just past the peak of the damage may prove to be useful in reducing transient enhanced diffusion of the lightly doped drain (LDD) or drain source implants. In general, as long as a low temperature process can be found to move the surface closer to the peak damaged region, the effect of TED will be reduced.

An example of a process other than etching which would move the surface closer to the damaged region is silicidation. In recent papers, Xu et. al. [32-33] has shown that platinum silicidation reduces TED of underlying boron-doped layers caused by arsenic implant. In one of their experiments, $3x10^{14}$ cm^{-2} arsenic was implanted at an energy 50 keV, over a boron doped SiGe layer through a 200Å screen oxide. When the sample was

annealed at 850°C, the diffusion length of the boron profile was very large. However, when Pt silicidation was performed prior to annealing, the sample exhibited a much less than TED. In order to explain this result, Xu et. al. proposed the use of a vacancy injection mechanism by Pt silicidation.

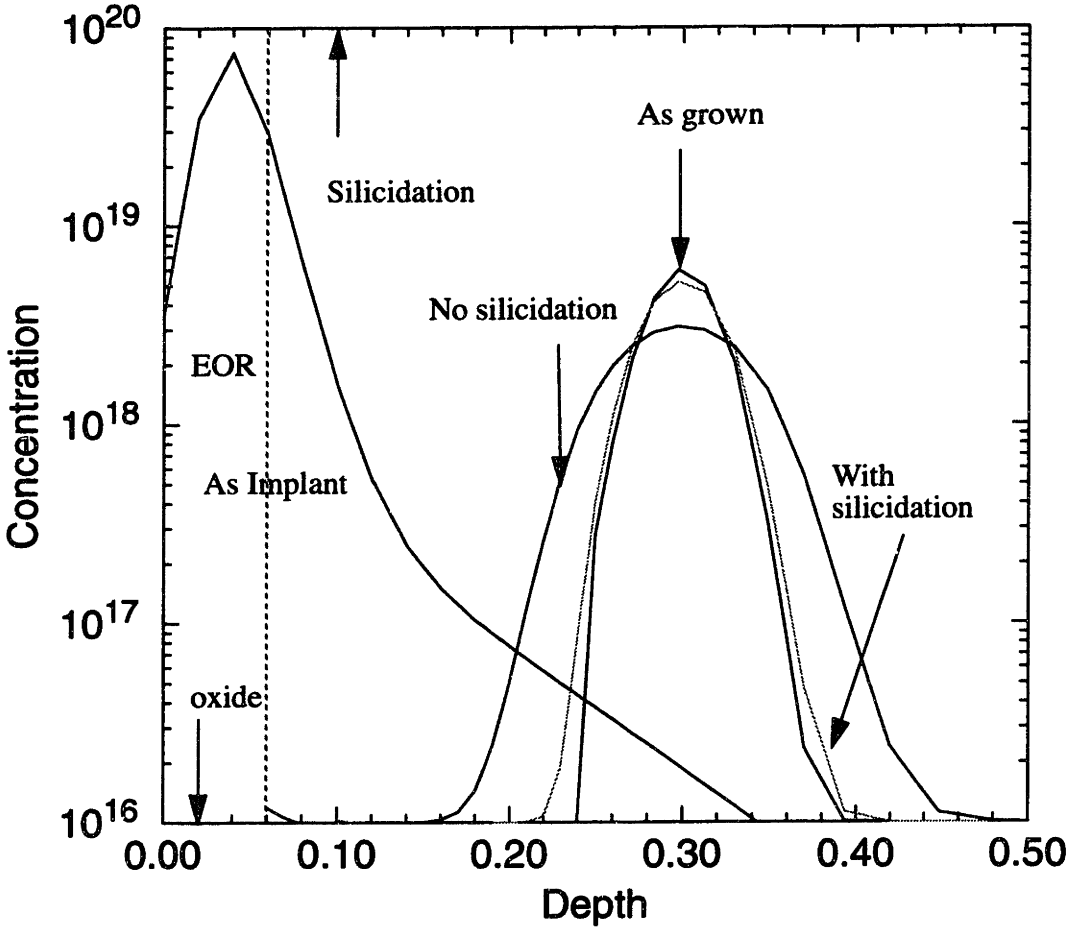

Figure 4.7: Simulation of the Pt silicidation experiment by Xu et. al. [33].

In order to test their hypothesis, in light of the findings in this chapter, Xu's experiment was modeled in PROPHET. In order to use the values of D_I and C_I extracted in this thesis, the D_I and C_I values at 800°C were transformed using activation energies of 2.44 eV and 2.36 eV [23] into values for use in PROPHET at 850°C. The large value of K_{surf} activated

by 2.44eV was also used in this simulation. Thus an important assumption was made here -- that the recombination velocity of the silicon/silicide interface was similar to that of the bare silicon surface.

In order to model damage distribution in this experiment, the +1 model was used. However, there is a caveat to this assumption--the As implant is amorphising. Thus, to correctly model the amorphization, it was assumed that the end of range damage (i.e. the original amorphous crystalline interface) was 600 Å from the surface of the oxide or 400Å from the surface of the silicon. Furthermore, it was assumed that the EOR damage would be a good sink for interstitials and that only damage past this amorphous crystalline interface was important. The effect of the silicon consumption due to PtSi formation is two-fold; it directly removes 80% of the damage created by implantation; furthermore it brings the surface into closer proximity to the remaining damage. The results in the simulation show that there is a dramatic fourteen fold reduction in the net diffusion enhancement of boron. This corresponds to a reduction of 3.7 in the diffusion length of boron, which could be used explain Xu's data. Unfortunately it is difficult to quantify the reduction in Xu's experiment since a significant portion of the boron diffusion occurred in the SiGe layer.

Thus it is possible that the increased surface proximity of the damage coupled with a large reduction in the damage, reduced the TED effect. This possibility would, in turn, imply that the vacancy injection mechanism is not important in this experiment.

Chapter 5

Vacancy Injection with Oxidation in the Presence of NF_3

5.1 Overview

Recent work has shown that oxidation in the presence of part per million levels of NF_3 results in oxidation retarded diffusion (ORD) of boron at a temperature of 1100 °C [44] and rapid shrinkage of oxidation induced stacking faults (OSFs) at temperatures between 900°C and 1100 °C [45]. Based on this data, Jaccodine et. al. has proposed that the presence of NF_3 changes oxidation from an interstitial injecting process to a vacancy injecting one.

It is hoped that this injection of vacancies during fluorinated oxidation will reduce the number of interstitials during oxidation and remove damage rapidly after implant. This might neutralize the effects of both TED and OED and result in faster lower temperature activation. For the suppression of TED to succeed, two processes must occur. The first is that sufficient vacancies must be injected to reduce the interstitials back to their equilibrium level i.e. to bring C_I to approximately C_I^*. Secondly, the vacancy and interstitial components must reach equilibrium faster than the time it takes for the point defects to affect diffusion.

Two different oxidizing ambients were considered, O_2 and N_2O [46]. The reason why N_2O was considered was because recent work has shown that gate oxidation in N_2O improves gate oxide characteristics [47]. However, no study has been made to examine the effect of N_2O oxidation on the underlying boron profiles.

5.2 Experimental Procedure

5.2.1 Effect of NF_3 oxidation on OED

The purpose of this experiment is to study the effects of N_2O oxidation and the effects of adding NF_3 to the oxidation ambient on the diffusion of underlying boron profiles. Although ORD of boron has been observed at high temperatures, the low temperature effect of the addition of NF_3 to the ambient has not been measured.

In addition, knowledge of oxidation enhanced or retarded diffusion (OED or ORD) of N_2O is important in process integration because the dopant profile under the gate oxide determines the threshold voltage of an MOS device.

The starting wafers were 5 inch 10-20 Ω cm <100> n-type wafers. BF_2 is implanted at an energy of 10 keV and a dose of $2x10^{13}$ cm $^{-2}$ with a tilt of 7° and rotation of 30°. The wafers are then annealed in Ar at 970°C for 10 min to remove the effect of TED from the experiment. Oxides were grown in the AG furnace at 50% O_2 + 50% Ar, 50% N_2O + 50% Ar, 50% O_2 + 50% Ar with 100 ppm NF_3 and 50% N_2O + 50% Ar with 100 ppm NF_3 at a pressure of 70 Torr at 970°C to a target thickness of 70Å. A control wafer was annealed in Ar for the time of the longest anneal, while a second control received no subsequent anneal following the TED anneal. Oxide thicknesses were measured with an ellipsometer and boron profiles were determined using Secondary Ion Mass Spectroscopy (SIMS). The implants were chosen to ensure that the peak concentration of boron was lower than n_i at 900°C.

5.2.2 Effect of NF_3 oxidation on TED

The purpose of this experiment is to determine if the effect of vacancy injection by oxidation in the presence of NF_3 is sufficient to suppress TED.

The samples received non amorphising low dose implants with the peak concentration of boron below n_i. Boron was implanted with a dose of $2x10^{14}cm^{-2}$ and energy of 10 keV. The wafers were then given a clean and a 2 minute 100:1 HF dip. This was followed by a 10 second rapid thermal anneal in either Ar or 50% Ar with 100 ppm NF_3 + 50% O_2 at a temperature of 900°C or 1100°C. The rapid thermal anneals were done at 70 Torr. Finally, the samples received an 800°C anneal for 2 hours.

An implant control was split from the lot after the implant and anneal controls for each element of the time-temperature matrix was split after the RTA step.

The 800°C anneal models any subsequent thermal anneals which may follow in VLSI processing. In addition, any remaining TED effects which haven't been annealed out in the 10 sec anneal, will become apparent in this 2 hour 800°C anneal.

In order to extract the diffusion coefficient of the boron profiles, SIMS profiling was used.

5.3 Results of NF_3 experiments

5.3.1 Effect of NF_3 oxidation on OED

Oxide Growth Rate

All the oxides were grown to within 5% of the target thickness of 70Å with the exception of the oxide grown in N_2O which had a thickness of 85Å. Thus the oxidation rate in N_2O was faster than in O_2. This is surprising since it is well known that N_2O oxides grow slower than O_2 at atmospheric pressure. In fact independent runs of N_2O oxides on the same RTA machine at atmospheric pressure indicates that the N_2O oxides grow much slower than O_2 at 1 atmosphere. Thus, at low pressure the relative oxidation kinetics of N_2O and O_2 reverses.

As is expected from previous results by Jaccodine et. al. [44], NF_3 greatly accelerates the rate of oxide growth. However, the presence of NF_3 accelerates the oxidation rate in dry oxygen more than in the N_2O ambient.

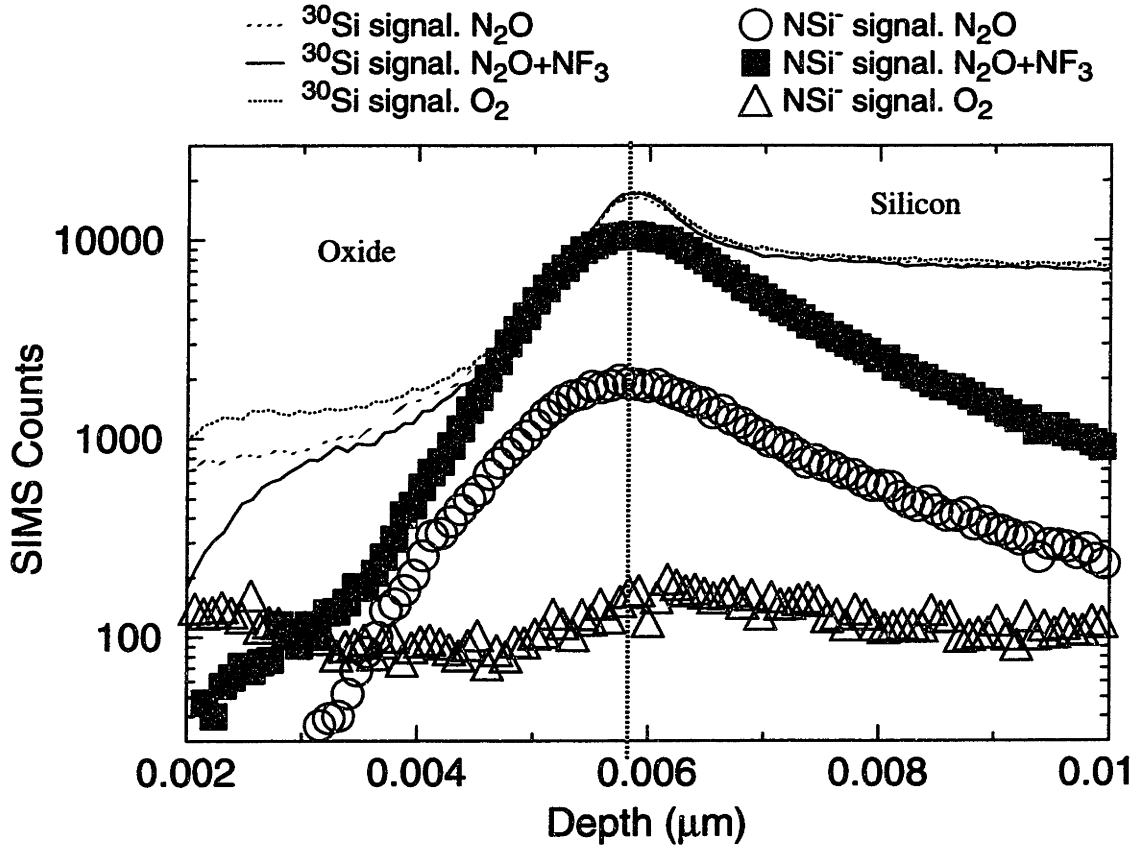

Figure 5.1: SIMS analysis of the nitrogen distribution in the N_2O grown oxides. The N distribution in the O_2 grown oxide is included for comparison. The profiles have been shifted so that the oxide/silicon interface line up.

The SIMS analysis in figure 5.1 shows a large nitrogen peak at the interfacial region for both oxides grown by N_2O, with and without NF_3. This nitrogen peak, which is absent in the O_2 grown oxide, is larger for the oxide grown in N_2O with NF_3 than for the oxide grown without NF_3. Unfortunately, this analysis is not quantitative since there are usually large SIMS artifacts associated with oxide/silicon interfaces. This interfacial nitrogen

peak is of interest since many of the useful properties of N_2O oxides are attributed to the build up of nitrogen at the interfacial region. However, it is interesting to note that despite the presence of this nitrogen "barrier", there is a 15x enhancement in the rate of oxidation with the presence of NF_3 in the N_2O ambient. Thus the reason why oxidation occurs slower in N_2O at one atmosphere is probably not due simply to the nitrogen at the silicon/ oxide interface, as has been previously suggested [47].

Oxidation Enhanced Diffusion

Figure 5.2 shows that the boron profiles of the samples which had been annealed in N_2O and O_2 respectively are very similar. The profiles both reach a concentration of $10^{17}cm^{-3}$ at a depth of 2250Å. Thus N_2O causes oxidation enhanced diffusion of boron with the same enhacement factor as dry oxygen. Diffusion constants of boron have been extracted under oxidizing conditions in both oxygen and N_2O and these have been presented in table 5.1. The 10% extra enhancement in diffusivity of boron annealed in the N_2O ambient is probably due to the thicker oxide grown in this ambient.

Anneal ambient (70 Torr)	Time	Oxide thickness Å	Extracted diffusivity (cm^2s^{-1})	Remarks
Ar	38 min	native	$6.44x10^{-15}$	Let D_{inert} =$6.44x10^{-15}$ cm^2s^{-1}
50% O_2	38 min	70 Å	$2.6x10^{-14}$	$D/D_{inert} = 4$
50% N_2O	38 min	85 Å	$2.8x10^{-14}$	$D/D_{inert} = 4.4$
50% NF_3/O_2	80 s	70 Å		profile shift too small
50% NF_3/N_2O	150 s	70 Å		profile shift too small

Table 5.1: Diffusivities of boron in silicon in different ambients.

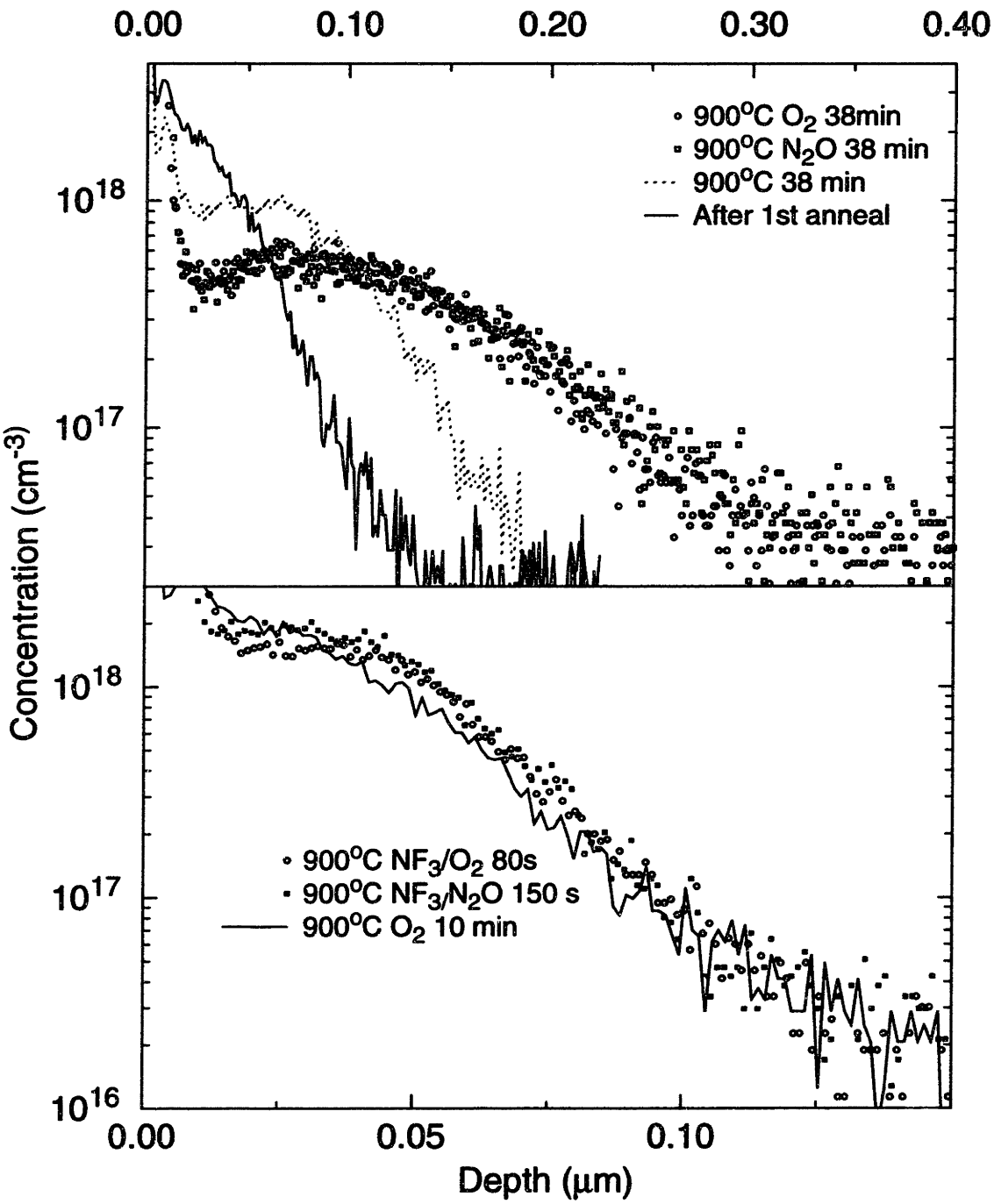

Figure 5.2: SIMS of OED experiment. All anneals were preceded by a 10 min Ar anneal to remove TED effects.

Figure 5.2 also shows that the addition of NF_3 to the oxidizing ambients of O_2 as well as N_2O eliminates oxidation enhanced diffusion. At a concentration of $10^{17}cm^{-3}$, the profiles move less than 40 Å from the starting profile, while an expected motion of about 200 Å is expected with an OED-enhanced diffusivity in 150s. The diffusivity of the boron layers could not be extracted with any accuracy for both N_2O and O_2 oxides grown in the presence of NF_3, because the profile shifts were layers could not be extracted with any accuracy for both N_2O and O_2 oxides grown in the presence of NF_3 because the profile shifts were too small.

It has been shown that the addition of ppm of NF_3 to O_2 in the oxidizing ambient at 1100°C will result in reduced the diffusion of boron profiles over that of the inert anneals [44]. Our results show independently that oxidation enhanced diffusion is suppressed even at lower temperatures which supports the conclusion that oxidation in the presence of NF_3 suppresses the injection of interstitials at low temperature.

The dielectric properties of the N_2O oxide grown in the presence of NF_3 should be studied in greater detail since it may provide a means of thermal oxide growth with negligible thermal budget but with useful oxide characteristics.

5.3.2 Effect of NF_3 oxidation on TED

The main result of this experiment is that NF_3 suppression of TED at 900°C is small and is summarized in figures 5.3 and 5.4. The SIMS results show that there is less TED in the ten second 900°C NF_3/O_2 anneal when compared to the ten second 900°C inert anneal. However, after the subsequent two hour 800°C anneal the two profiles were virtually the same. This suggests that the main effect of the NF_3 anneal was to slow down the transient diffusion effect, not suppress it. See figure 5.3.

More surprisingly, was the fact that addition of NF_3 increased the diffusivity of boron at 1100°C. The total boron motion, including transient diffusion, under NF_3/O_2 oxidizing conditions at 1100°C was 1.5 times that in the ambient condition. This is in contrast to Jaccodine's result that boron diffusivity was reduced under NF_3/O_2 oxidizing conditions. See figure 5.4. This result may be related to another result in this experiment, the significant diffusion observed in the sample which received the 1100°C inert ambient anneal. In fact the boron diffusivity was enhanced by an average factor of eight over the literature value.

It is possible that this "enhancement" is due to a lack of temperature control in the short high temperature anneal at 1100°C. The introduction of NF_3 might increase the thermal coupling between the lamp and the wafer. Since the system was run in open loop, this may have resulted in the 1.5 enhancement in the boron diffusivity for the sample annealed in NF_3. This hypothesis is supported by the unexpectedly large diffusivity of the sample annealed in the inert ambient which cannot be explained by TED, because the TED at 900°C (which is greater than that at higher temperatures according to every published study. See, for example, [37]) pushed the "junction" depth of boron to 1750Å, while at 1100°C, the "junction" moved to 2000Å.

However, in order to cause this large amount of diffusion, the real wafer temperature would have to be 1210°C. Such a large anneal temperature would be surprising for two reasons. The first is the magnitude of the error in temperature; a 100°C error in temperature would be more than expected. The second is that the large and extreme thermal budget might have thermal "shocked" the wafer, resulting in warpage. Furthermore, when a control inert ambient wafer was annealed at 1100°C for 10 s in another RTA machine run in close loop, (this is the same machine which was calibrated with the sample holder and

mentioned section 3.3.1) the resulting boron profile exhibited a similar large transient. Still, the results of the 1100°C experiment are, at best, inconclusive.

Finally there is significant tail diffusion at 900°C. In order to achieve the profile movements at lower concentrations, a diffusion enhancement of about 10^3 is required, although this large coefficient will also result in a much larger than observed diffusion at high concentrations. The shape of the profile -- small diffusion at high concentration coupled with large diffusion at low concentration -- is consistent with all the previous work done at 900°C [34-38].

5.4 Modeling TED of extrinsically doped boron profiles

A large part of this thesis was devoted to studying the effects of TED under intrinsic conditions to de-couple electric field effects from complicated point defect equations. However, many boron implants of technological importance are extrinsically doped, that is, they have peak concentrations which are much more than n_i. A common problem in the modeling of transient enhanced diffusion at temperatures of less than 1000°C in such boron profiles is that the enhancement in diffusion at high concentrations is much less than at lower concentrations. This effect can be observed directly from the boron profiles shown in figure 5.3. The inflection in boron profiles at the $1x10^{19}cm^{-3}$ level after the ten second 900°C anneal shows that the diffusivity of boron at concentrations below $10^{18}cm^{-3}$ is more than the diffusivity above $1x10^{19}cm^{-3}$.

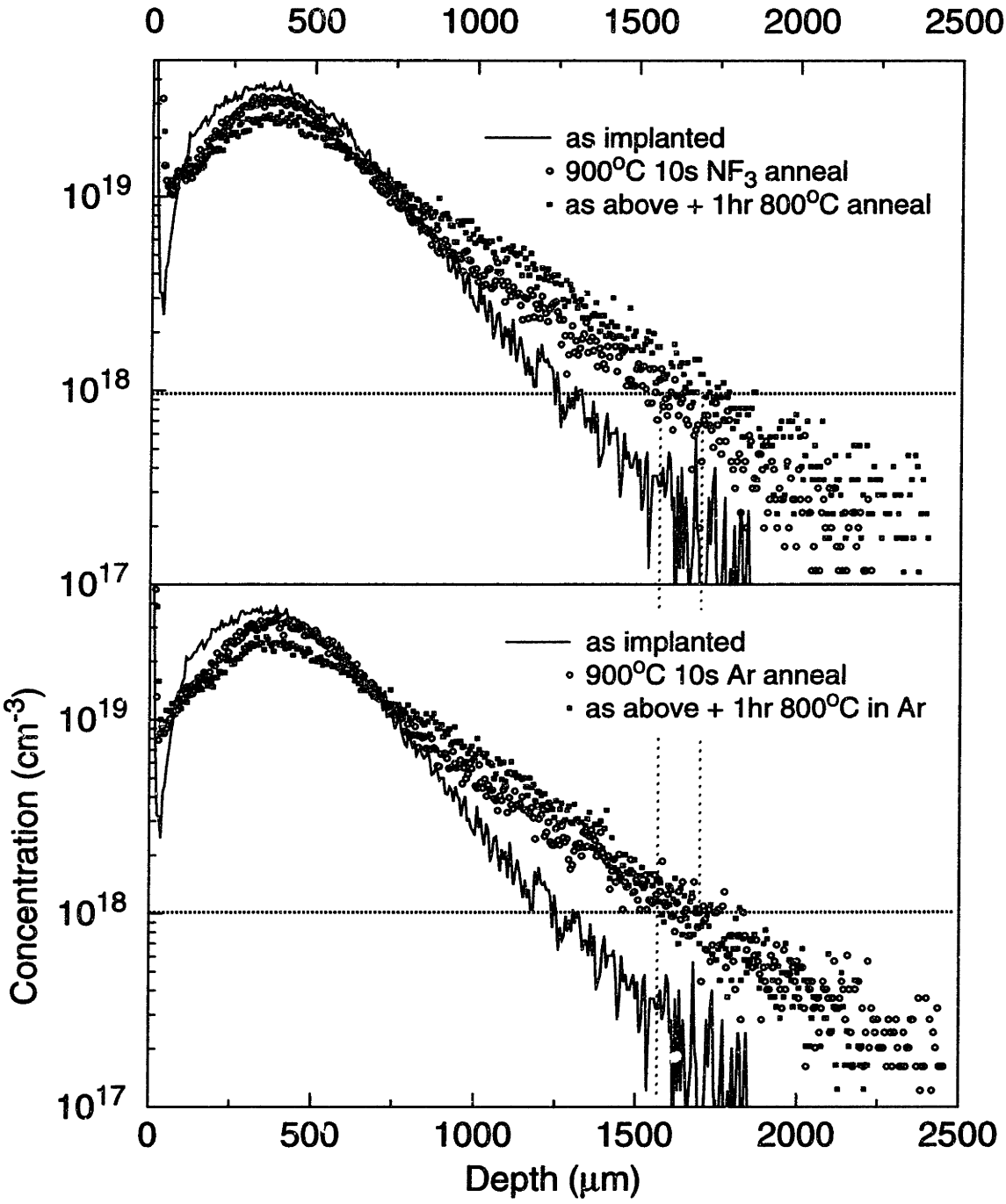

Figure 5.3: Effect of 900°C anneal in NF_3/O_2 on TED

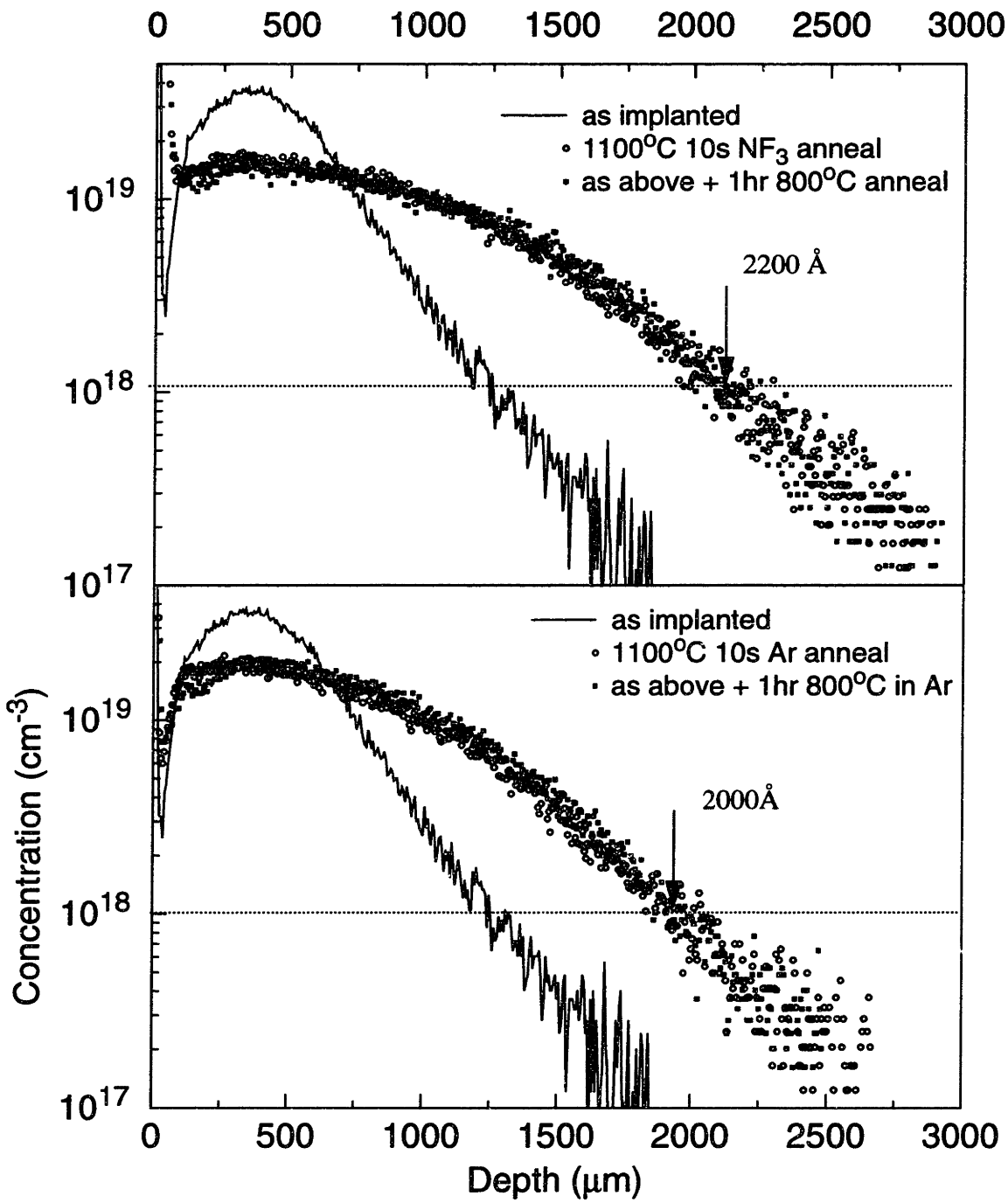

Figure 5.4: Effect of 1100°C anneal in NF_3/O_2 on TED

Several ideas have been proposed to explain this phenomenon. The first is a model in which damage due to the implant acts as trap for boron during diffusion. Since the peak damage in boron implants is coincident with the peak of the implanted boron distribution, this would explain the fact that above a critical doping concentration, boron exhibits significantly less diffusion than when it is in the low concentration part of the profile. However, this model doesn't explain Michel's observation that a deep stabilized boron marker exhibited this non-uniform enhancement behavior when a silicon damage implant was performed away from the marker [35].

The second is a pairing model in which the diffusion of boron is a result of a pairing of boron and interstitials. If there are insufficient numbers of interstitials to cause pairing of boron above 10^{18} cm^{-3}, then the net effect would be to decrease diffusion at higher concentrations. However, Griffin has argued that the pair distribution eventually leads to the same TED as if pairing had not occurred [24].

A third model is interstitial induced boron clustering which has been proposed by Griffin [24] and Stolk [40]. In this model, a combination of a high concentration boron and a high concentration of silicon interstitials cause the boron to cluster, which in turn causes large reductions in the effective diffusivity.

Based on this idea, I developed an empirical clustering model for extrinsically doped boron profiles and found reasonable fits to data from various sources. In this model, the active boron concentration, C_{active}, is assumed to take the form:

$$C_{total} = C_{active} + \beta C_{active}^{m} \tag{5.1}$$

which resembles the solid solubility model used for arsenic by Fair and Weber [48]. In order to determine the values of m and β, data from [34, 36, 37, 38 and 39] and the NF_3 TED anneals presented in this work were fitted. The data covered a temperature range

from 800°C to 1000°C, boron doses from 10^{13} cm^{-2} to $5x10^{15}$ cm^{-2} and energy from 5 keV to 80 keV. Good fits were obtained with m=3 and $\beta=4.38x10^{-48}$ exp(2.352/kT) over this data set. See figure 5.5-5.8. Solid solubility considerations can also be taken into account by turning on the solid solubility model after the transient anneal (figure 5.9).

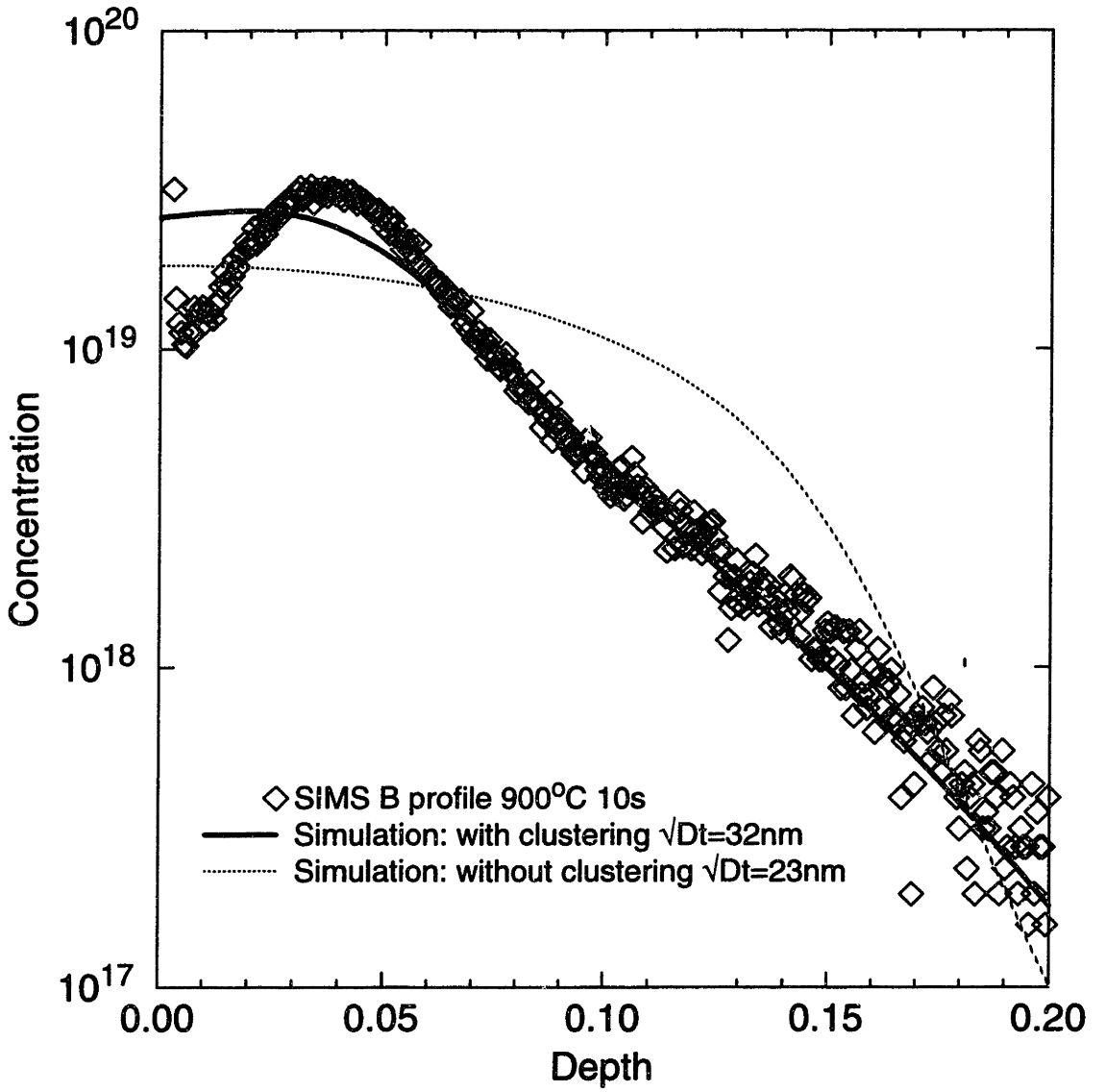

Figure 5.5: Figure showing fit of TED in the NF_3 TED experiment. The simulation with clustering is a much better fit to the data.

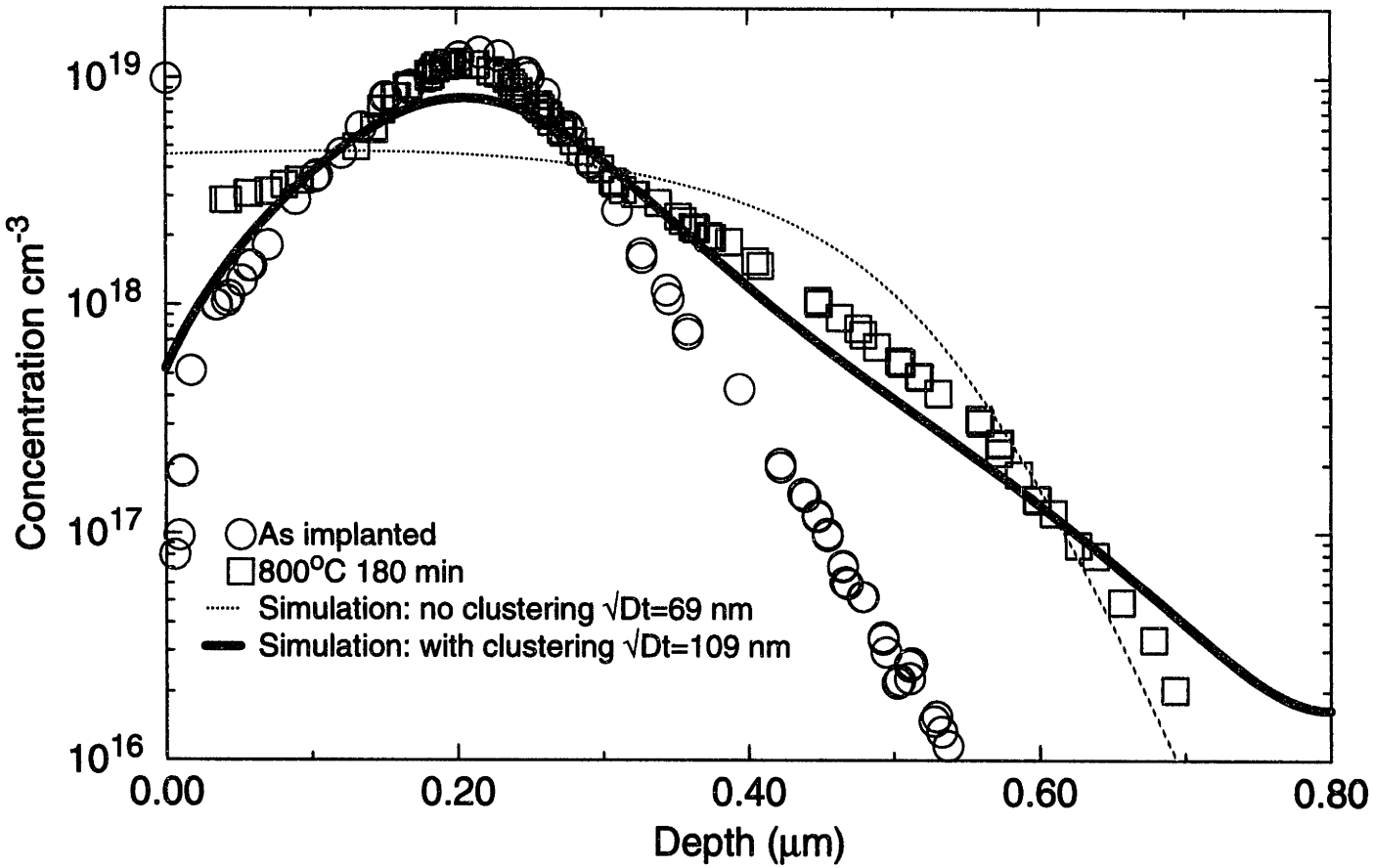

Figure 5.6: Figure showing the fit at 800°C. Data from Michel et. al. Boron was implanted at an energy of 60 keV and dose of $2x10^{14}$ cm^{-2}.

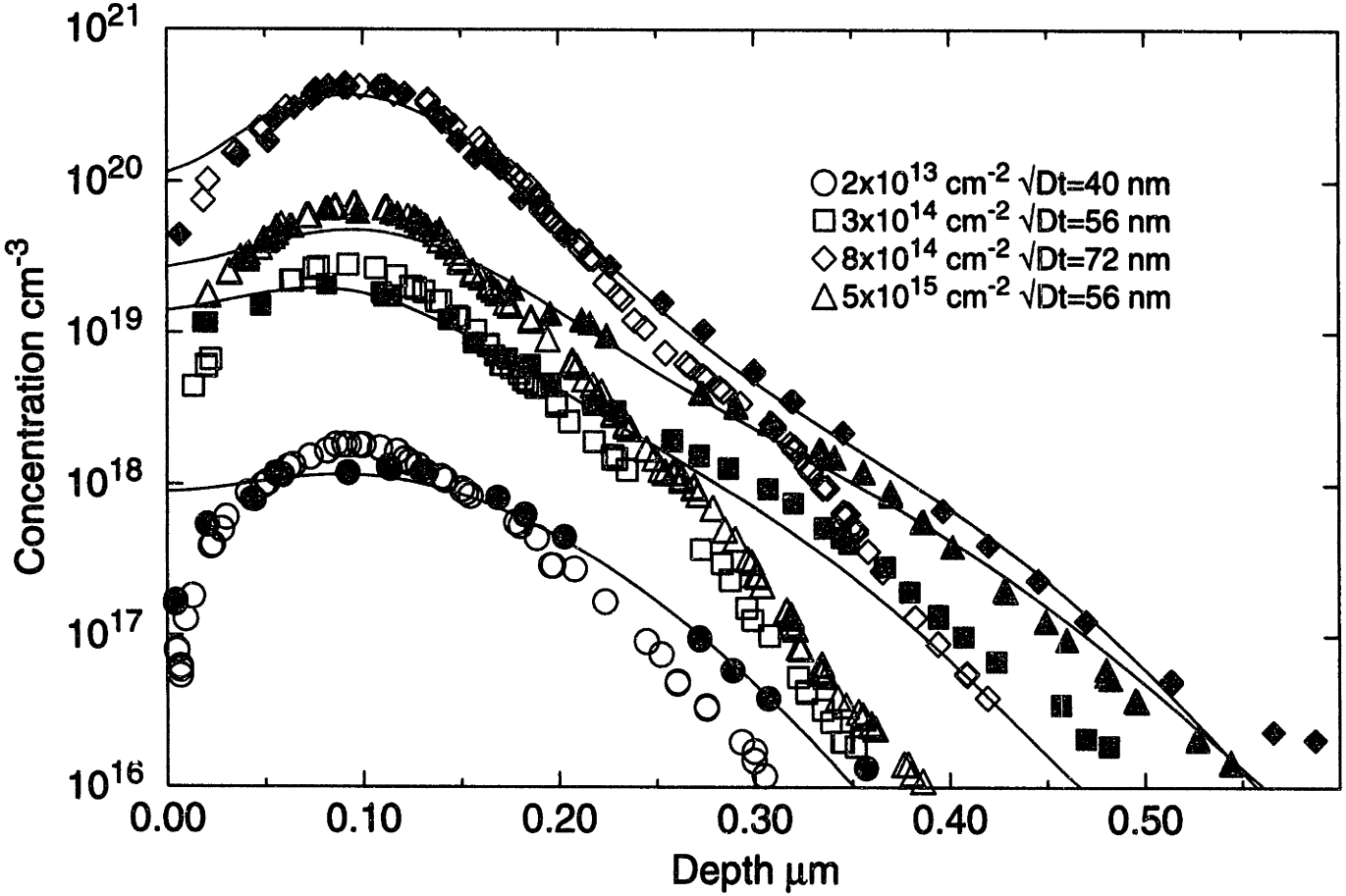

Figure 5.7: Graph showing fits to various doses. The anneal was 900°C for 15 min and implant energy=25keV. Open symbols are as-implanted SIMS profiles, filled symbols are annealed. Solid lines are simulations. Data from Cowern et. al.

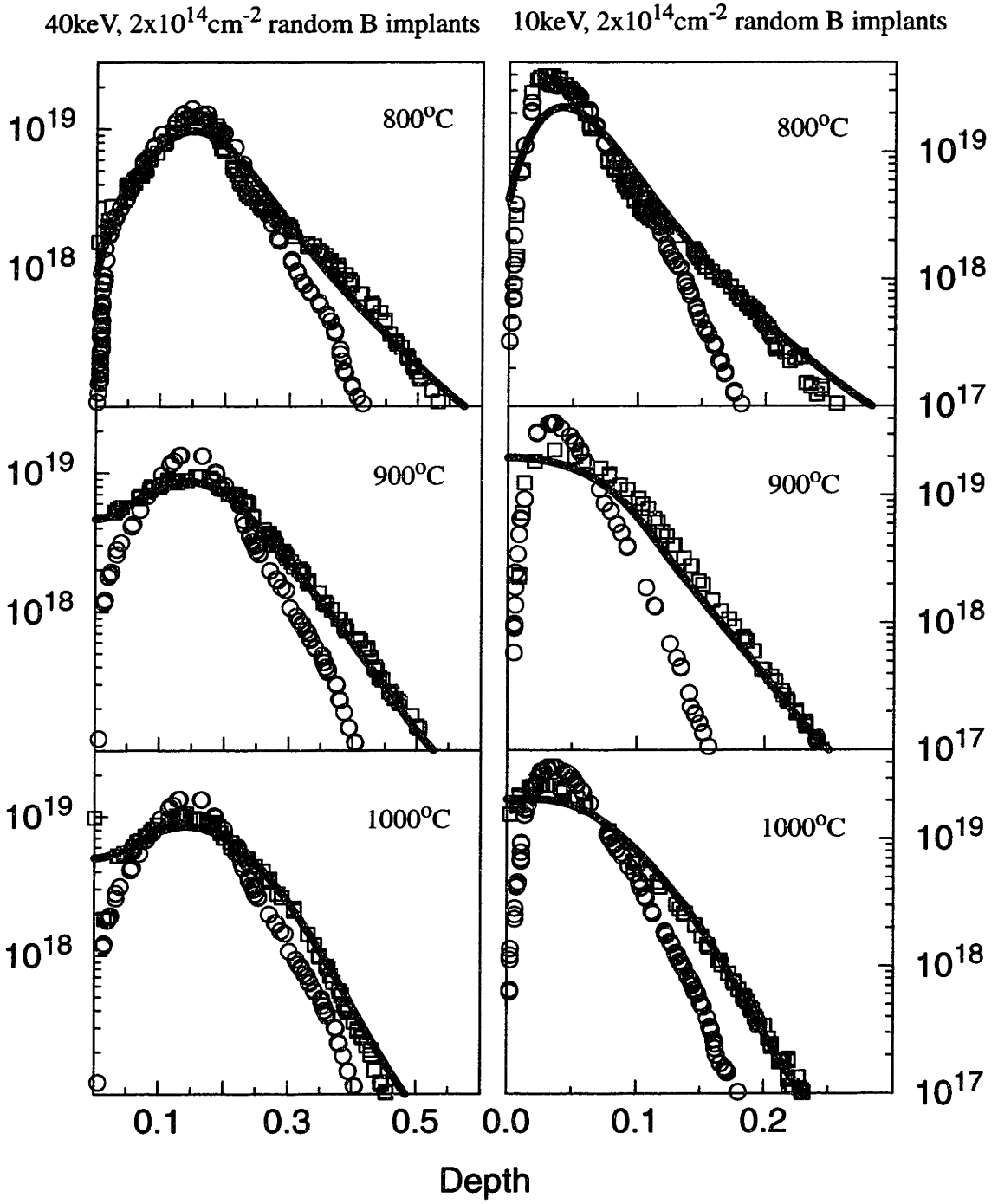

Figure 5.8: Fits using the clustering model. Data from Chu et. al. [38]. The circles represent the as implanted profile, while the squares represent diffused profile. The solid black line is the simulated fit.

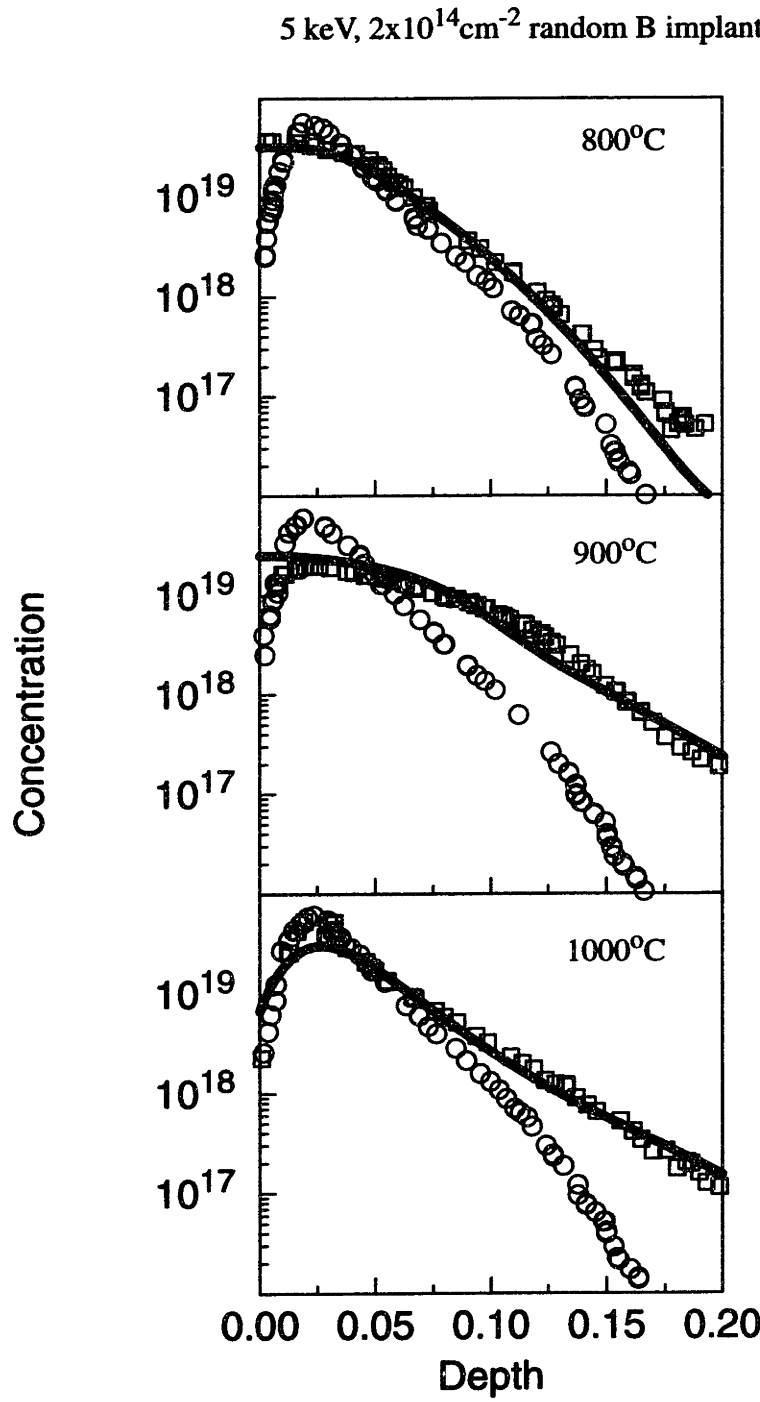

Figure 5.8 cont'd: Fits to the 5keV data by Chu et. al.

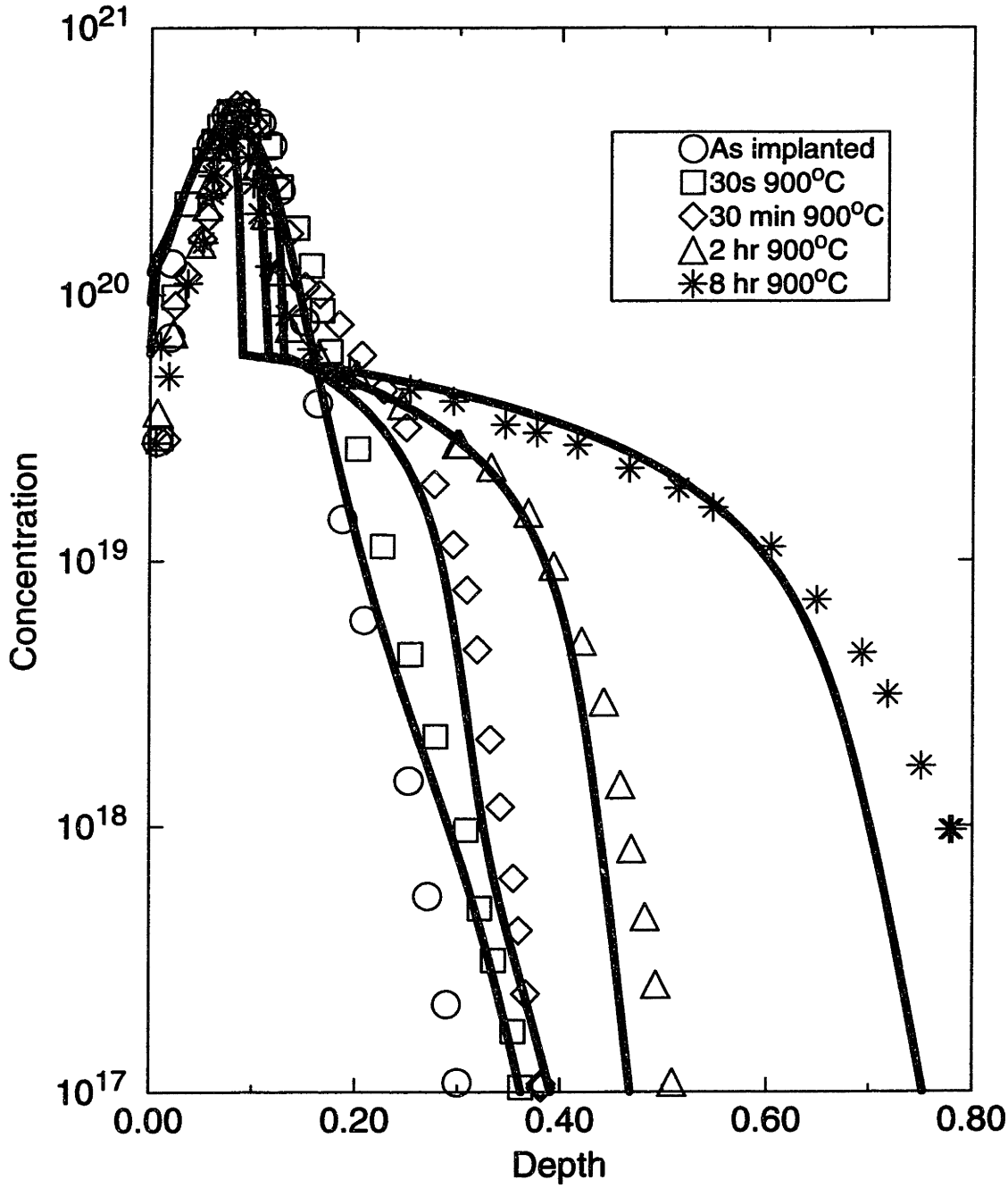

Figure 5.9: Simulation of long post implant anneals. The clustering model was turned off and the solid solubility model was turned after 1 min. Data from Solmi et. al. [37]

Chapter 6

Conclusions and Future Work

6.1 Conclusions

Diffusion of boron in silicon at 800°C was studied for very short times to throw some light on the development of the diffusion transient following ion implantation.

This study showed that transient enhanced diffusion (TED) proceeds at a steady rate even at the shortest times. The rate was about 6000 times higher than the equilibrium diffusion rate at the same temperature.

A deep boron marker moved at the same rate as a shallow boron marker, leading to the conclusion that the species mediating transient diffusion, the interstitial, is very mobile. Thus, the interstitial diffusivity must be at least $1x10^{-9}$ cm^2/s in this CVD grown material.

The high mobility and steady supersaturation of interstitials suggest that interstitial clustering must be taken into account when modeling transient diffusion. Without a mechanism to hold the interstitials in place, the high mobility would rapidly reduce the interstitial supersaturation.

In another study, etching the surface to bring the surface into the closer proximity to the damage was shown to reduce the amount of transient diffusion. This result supports the idea that the surface is the predominant annealing site of damage after transient diffusion. A high surface recombination rate for interstitials, within at least 0.005 of the diffusion-limited value, is necessary to model this result.

Oxidation enhanced diffusion (OED) of boron under N_2O and NF_3 ambients was measured in the final experiment. N_2O oxidation results in the same diffusion enhancement as O_2 oxidation. The addition of trace amounts of NF_3 to the oxidizing ambient suppressed

OED in both N_2O and O_2 ambients, without changing significantly the nitrogen at the peak. However, oxidation in the presence of NF_3 did not suppress TED.

In order to explain the shapes of the profiles in the experiments, a boron clustering model was developed, similar to conventional solubility models, but using a lower "transient" solubility. This empirical clustering model was shown to give good fits to low temperature TED profiles in the literature.

6.2 Future work

The time evolution of TED should be studied more carefully with narrower markers. This would enable more accurate determinations of K_{clust} and D_I. In addition, the experiment needs to be repeated at a range of temperatures, so that the temperature variation of these values can be studied.

The damage distribution caused by ion implantation is still not well understood and must be studied in greater detail to improve the accuracy of point defect models. Although the +f model used in this thesis is extremely useful in analyzing the physical mechanisms of transient diffusion, its predictive ability is inadequate since f is still a fitted parameter. Although the values of f used in analyzing the experiments presented here were all less than or equal to 1, a value of 10 has been reported as necessary to explain the full effects of TED in some situations [3]. Such large variances in f cannot be easily explained and are difficult to model. Furthermore, the +f model is unable predict important trends, like the large amount of TED at low doses and the saturation of TED at high implant energies.

Although a large value of K_{surf} has been determined on clean etched silicon, the values K_{surf} needs to be determined for interfaces between silicon and thin films such as oxides or silicides. Furthermore the effect of etching to the peak of a shallow boron profile should be studied as this may provide a useful way of reducing TED of profiles.

A point defect clustering model should be developed for the clustering mechanism. Although the empirical model could be very useful for extracting diffusion lengths of boron consistently and for quick empirical modeling, a point defect model will be needed to fully model effects transient diffusion, especially in situations where the damage is introduced separately from the profile.

References

[1] S. Wolf and R. N. Tauber, Silicon Processing for the VLSI Era, Vol I, (1986).

[2] Y. El-Mansy, IEEE Trans. Electron Devices, **ED-29**, 567 (1982).

[3] C. S. Rafferty, H.-H. Vuong, S.A. Eshraghi, M.D. Giles, M.R.Pinto and S.J.Hillenius, IEDM 93, 311, (1993).

[4] M. Servidori, R. Angelucci, F. Cembali, P. Negrini, S.Solmi, P. Zaumseil and U. Winter, J. Appl. Phys. **61**, 1834, (1987).

[5] R. B. Fair, IEEE Trans. on Electron Devices, **37**, 2237, (1990).

[6] T. E. Seidel and A. U. MacRae, Radiation Effects, **7**, 1 (1971).

[7] M. Miyake, S. Aoyama, J. Appl. Phys., **63**, 1754 (1988).

[8] M. Giles, J. Electrochem. Soc, **138**, 1160, (1991).

[9] L.A. Christel, J.F. Gibbons, and S. Mylroie, J. Appl. Phys., **51**, 6176 (1980).

[10] M.D. Giles and J.F. Gibbons, Nucl. Instrum. Meths., **209/210**, 33 (1983).

[11] N. E. B. Cowern, K T. F. Janssen, and H. F. F. Jos, J. Appl. Phys. **68**, 6191, (1990).

[12] R.J. Schreutelkamp, J.S. Custer, V. Raineri, W. X. Lu, J. R. Liefting and F. W. Saris, Materials Science and Engineering B, **12**, 307 (1992).

[13] S.D. Brotherton, J. R, Ayres, J. B. Clegg and J. P. Gowers, J. of Electronic Materials, **18**, 173 (1989).

[14] P. A. Packan, "Physics Modeling of Transient Diffusion Effects in Silicon due to Surface Oxidation and Ion-Implantation", PhD Thesis, Stanford University, (1991).

[15] P.M. Fahey, P.B. Griffin and J.D. Plummer, Review of Modern Physics, **61**, 289, (1989).

[16] S. M. Hu, J. Applied Phys., **45**, 1567, (1974).

[17] D. A. Antoniadis, A. G. Gonzalez and R. W. Dutton, J. Electrochem. Soc., **125**, 813, (1978).

[18] D. A. Antoniadis, J. Electrochem. Soc., **129**, 1093, (1982).

[19] C.S. Rafferty, unpublished.

[20] M. Javais, J. Avia, E. Rubia, L.A. Marques, L. Bailon and J. Barbolla, International Conf. on Ion Implantation Technology, (1994).

[21] H. Park and M. Law, J. Appl. Phys., **72**, 3431, (1992).

[22] H.-J. Gossman, C. S. Rafferty, H. S. Luftman, F. C. Unterwald, T. Boone and J. M. Poate, Appl. Phys. Lett., **63**, 639, (1993).

[23] G. Bronner and J. D. Plummer, J. Appl. Phys., **61**, 5286, (1987).

[24] P. B. Griffin, P. M. Fahey, J. D. Plummer and R. W. Dutton, Appl. Phys. Lett., 47, **319**, (1985).

[25] N.A. Stolwijk, B. Schuster, and J. Hölzl, Appl. Phys. A **33**, 133 (1984).

[26] P. Fahey, R.W. Dutton, and S.M. Hu, Appl. Phys. Lett. **44**, 77 (1984).

[27] A. F. Burenkov, Tables of Ion Implantation spatial distributions, Gordon and Breach, (1986).

[28] J.F. Zeigler, J.P. Biersack, and U. Littmark, The Stopping and Range of Ions in Solids, Pergamon Press, New York (1987)

[29] Y. Kim, H. Z. Massoud and R. B. Fair, J. Electronic Materials, **18**, 143 (1989).

[30] E. Gannin and A. Marwick, Matl. Res. Soc. Symp. Vol. **147**, 13, (1989).

[31] J. Narayan and K. Jagannadham, J. Appl. Phys., **62**, 1694, (1986).

[32] D.-X. Xu, C.J. Peters, J. McCaffrey, S. J. Rolfe, J.-P. Noël, and N.G. Tarr, VLSI Symposium, (1994).

[33] D.-X. Xu, C.J. Peters, J. McCaffrey, S. J. Rolfe, J.-P. Noël, and N.G. Tarr, Appl. Phys. Lett. **64**, 3270, (1994).

[34] A. E.Michel, Material Res. Symp. Proc, **52**, 3 (1986).

[35] A.E. Michel, Appl. Phys. Lett., 51, 487, (1987).

[36] R.Angelucci, F. Cembali, P. Negrini, M. Servidori, and S. Solmi, J. Electrochem. Soc., **134**, 3130, (1987).

[37] S. Solmi, F. Barufuldi and R.Canteri, J. Appl. Phys., **69**, 2135, (1991).

[38] W.K. Chu, M.Z. Numan, J.Z. Zhang, G.S. Sandhu and A.E. Michel, Nuclear Instruments and Methods in Physics Research, **B37/38**, 365 (1989).

[39] P.B. Griffin, R.F. Lever, R.Y.S. Huang, H.W. Kennel. P.A. Packan and J.D. Plummer, IEDM 93, 295 (1993).

[40] P. Stolk, to be published

[41] T. E. Seidel, D. J. Lischner, C. S. Pai, R. V. Knoell, D. M. Maher and D. C. Jacobson, Nuclear Instruments and Methods in Physics Research, **B7/8**, 251, (1985).

[42] J. Ahn, W.Ting, T.Chu, S. N. Lin, and D. L. Kwong, J. Electrochem. Soc. **138**, L39 (1991).

[43] K. Ohyu, T.Hoga, Y.Nishioka and N. Natsuaki, Jpn. J. Appl. Phys. **28**, 1041 (1991).

[44] U.S. Kim, T. Kook and R. J. Jaccodine, J. Electrochem. Soc. **137**, 2296 (1988).

[45] U.S. Kim and R. J. Jaccodine, Appl. Phys. Lett., **49**, 1201 (1986).

[46] J.G. Huang and R.J. Jaccodine, J. Electrochem. Soc., **140**, L15 (1993).

[47] J. Ahn, W. Ting, T. Chu, S. N. Lin and D. L. Kwong, J. Electrochem. Soc., 138, L39 (1991).

[48] R. B.Fair and G. R. Weber, J. Appl. Phys., **44**, (1973) 273.